

Modification of the high latitude ionosphere F region by X-mode powerful HF radio waves: Experimental results from multi-instrument diagnostics

N. F. Blagoveshchenskaya ¹, T. D. Borisova ¹, T. K. Yeoman ², I. Häggström ³, A.S. Kalishin ¹

¹ Arctic and Antarctic Research Institute, St. Petersburg, 199397, Russia, nataly@aari.nw.ru

² Department of Physics and Astronomy, University of Leicester, Leicester LE1 7RH, UK

³ EISCAT Scientific Association, Kiruna, SE-961 28, Sweden

Correspondence and proofs should be sent to Dr. N. F. Blagoveshchenskaya

Address: Arctic and Antarctic Research Institute, 38, Bering str., St. Petersburg, 199397, Russia

e-mail: nataly@aari.nw.ru

1 **Abstract.** We present experimental results concentrating on a variety of phenomena in
2 the high latitude ionosphere F2 layer induced by an extraordinary (X-mode) HF pump wave at
3 high heater frequencies ($f_H = 6.2 - 8.0$ MHz), depending on the pump frequency proximity to the
4 ordinary and extraordinary mode critical frequencies, foF2 and fxF2. The experiments were
5 carried out at the EISCAT HF heating facility with an effective radiated power of 450 – 650 MW
6 in October 2012 and October – November 2013. Their distinctive feature is a wide diapason of
7 critical frequency changes, when the $f_H / foF2$ ratio was varied through a wide range from 0.9 to
8 1.35. It provides both a proper comparison of X-mode HF-induced phenomena excited under
9 different ratios of $f_H / foF2$ and an estimation of the frequency range above foF2 in which such X-
10 mode phenomena are still possible. It was shown that the HF-enhanced ion and plasma lines are
11 excited above foF2 when the HF pump frequency is lying in a range between the foF2 and fxF2,
12 $foF2 \leq f_H \leq fxF2$, whereas small-scale field-aligned irregularities continued to be generated even
13 when f_H exceeded fxF2 by up to 1 MHz and an X-polarized pump wave cannot be reflected from
14 the ionosphere. Another parameter of importance is the magnetic zenith effect (HF beam/radar
15 angle direction) which is typical for X-mode phenomena under $f_H / foF2 > 1$ as well as $f_H / foF2 \leq$
16 1. We have shown for the first time that an X-mode HF pump wave is able to generate strong
17 narrow band spectral components in the SEE spectra (within 1 kHz of pump frequency) in the
18 ionosphere F region, which were recorded far away from the HF heating facility. The observed
19 spectral lines can be associated with the ion acoustic, electrostatic ion cyclotron, and electrostatic
20 ion cyclotron harmonic waves (otherwise known as neutralized ion Bernstein waves). It is
21 suggested that these spectral components can be attributed to the stimulated Brillouin scatter
22 (SBS) process. The comparison between the O- and X-mode narrow band spectra clearly
23 demonstrated that only an X-polarized pump wave scattered by SBS can propagate more than
24 one thousand km without significant deterioration.

25

26 **Keywords.** Ionosphere (Active experiments), Radio Science (Nonlinear phenomena)

27

28 1. Introduction

29

30 HF pumping experiments in the ionospheric F-region are most commonly conducted with
31 the use of high-power HF radio waves with ordinary polarization (O-mode). An O-polarized HF
32 pump wave effectively interacts with the background ionosphere plasma in the F2 layer in the
33 region between the HF reflection height and upper hybrid resonance altitude leading to the
34 excitation of thermal parametric (resonance) and parametric decay instabilities, which produce a
35 wide variety of phenomena (see, for example, Erukhimov et al., 1987; Robinson, 1989; Stubbe,
36 1996; Gurevich, 2007 and references therein). As for an X-mode HF pump wave, it does not
37 match the resonance altitudes and, therefore, should not excite the thermal parametric
38 (resonance) instability (TPI) as well as the parametric decay instability (PDI). However, an X-
39 polarized HF pump wave can produce the differential ohmic heating on electrons (Gurevich,
40 1978; Lofas et al., 2009; Kuo et al., 2010). The electron thermal pressure force leads to the
41 generation of artificial large-scale irregularities because of the growth of a self-focusing
42 instability of an electromagnetic HF wave beam (Dunkan and Behnke, 1978; Gurevich, 1978;
43 Farley et al., 1983; Kuo et al., 2010; Frolov et al., 2014).

44 An X-polarized HF pump wave cannot match the resonance altitude thus only an O-mode
45 wave is able to generate small-scale field-aligned artificial irregularities (FAIs). Indeed, EISCAT
46 HF heating experiments have demonstrated that at a heater frequency of $f_H = 4.544$ MHz, which
47 was below the maximum plasma frequency f_oF2 , the change of polarization to X-mode led to the
48 disappearance of FAIs, observed under O-mode heating (Robinson et al., 1997). The opposite
49 behavior of FAIs was found at heater frequencies lying above the f_oF2 ($f_H / f_oF2 \geq 1$).
50 Blagoveshchenskaya et al. (2011a; 2011b) have shown for the first time that at heater
51 frequencies lying in the range of 4.0 – 5.4 MHz, an X-polarized HF pump wave, injected parallel
52 to the magnetic field line at frequencies $f_H \geq f_oF2$, can excite strong small-scale field-aligned
53 artificial irregularities responsible for backscatter measured by the CUTLASS radars. Detailed

54 studies of the X-mode FAI properties, with the spatial size across the geomagnetic field of $l_{\perp} \approx 11$
55 – 15 m, from a large number of EISCAT experiments at different heater frequencies of 4.040,
56 4.544, 4.9128 and 5.423 MHz have demonstrated that such FAIs were observed in a frequency
57 band of about 1.2 MHz above the maximum plasma frequency foF2 (Blagoveshchenskaya et al.,
58 2013). The experiments reported by Blagoveshchenskaya et al. (2011a; 2013) were carried out in
59 the afternoon and evening hours in quiet magnetic conditions under an effective radiated power
60 of 75-180 MW with the HF array having a beam width of 12° at the -3 dB point. Further
61 investigations of X-mode HF-induced phenomena at EISCAT were carried out at high heater
62 frequencies ($f_H > 6.0$ MHz) with an effective radiated power of about 450 – 650 MW and a
63 heater beam width of 5° . They have shown evidence for strong plasma modifications even when
64 the heater frequency was below foF2. It was found that at high heater frequencies the artificial
65 optical emissions at red and green lines accompanied with HF-enhanced ion and plasma lines
66 and strong FAIs can be excited in the F-region of the high latitude ionosphere under X-mode HF
67 pumping towards the magnetic zenith at heater frequencies lying mainly below the foF2
68 (Blagoveshchenskaya et al., 2014). When $f_H \leq \text{foF2}$, O-mode leakage effects cannot be
69 completely excluded. The only heater pulse under f_H lying above foF2 considered by
70 Blagoveshchenskaya et al. (2014), differed in pulse duration and background conditions.
71 Because of that the X-mode phenomena excited above foF2 require further clarification.
72 Moreover, this heater pulse gave no opportunity for the determination of the frequency range
73 above the foF2 in which various X-mode HF-induced phenomena are generated.

74 This paper provides further insight into unresolved issues associated with X-mode
75 pumping the high latitude ionospheric F-region by the EISCAT HF heating facility at high heater
76 frequencies ($f_H = 6.2 - 8.0$ MHz). The key parameter considered during the observations is the
77 ratio of the heater frequency to the O- and X-mode critical frequencies. The main attention is
78 paid to the detailed investigation of the X-mode phenomena excited at high heater frequencies
79 lying above the maximum plasma frequency, when the “pure” X-mode phenomena can be

80 generated and the O-mode leakage effects are impossible. We analyze the behavior of HF
81 enhanced ion and plasma lines (HFIL, HFPL), electron density modification, and artificial field-
82 aligned irregularity production depending on the pump frequency proximity to the critical
83 frequencies.

84 In order to investigate the magnetic zenith effect observed under X-mode pumping, we
85 discuss experimental data obtained under different HF incidence angle of the Tromsø HF heating
86 facility accompanied by elevation angle stepping the EISCAT UHF radar between 72° and 90°
87 (HF beam/radar angle direction).

88 Finally, we demonstrate the first evidence of the generation of distinct narrow band
89 spectral components in the stimulated electromagnetic emission (SEE) spectra within 1 kHz of
90 the pump frequency induced by an X-mode HF pumping. These spectral components, which can
91 be associated with the ion acoustic (IA), electrostatic ion cyclotron (EIC), and ion Bernstein (IB)
92 waves, were recorded at a distance of about 1200 km away from the EISCAT HF Heating
93 facility.

94

95 **2. Experimental description and instrumentation**

96

97 HF pumping experiments have been carried out during Russian EISCAT campaigns
98 during October -November 2013 and October 2012 in quiet magnetic conditions and high solar
99 activity in the afternoon and evening hours between 14 and 18 UT. Artificial perturbations in the
100 high latitude ionosphere F2-layer were created by the EISCAT HF Heating facility (69.6° N,
101 19.2° E; magnetic dip angle $I=77^\circ$). We will consider in detail the observational results obtained
102 in the course of experiments on 27 and 28 October, 2 and 3 November 2013 and 21 October
103 2012. Much of the EISCAT heating campaign from 18 October to 3 November 2013 was
104 described by Blagoveshchenskaya et al. (2014).

105 Multi-instrument diagnostics were used for the investigation of the X-mode HF-induced
106 phenomena at high pump frequencies ($f_H = 6.2 - 7.953$ MHz) depending on the ratio of heater
107 frequency to the maximum plasma frequency when the f_H / f_oF2 ratio was varied through a range
108 from 0.9 to 1.35. The EISCAT UHF incoherent scatter radar at 930 MHz, spatially co-located
109 with the HF heating facility at Tromsø, has been applied in the evaluation the ionospheric plasma
110 parameters and HF-enhanced ion and plasma lines (HFILs and HFPLs) from the backscattered
111 radar spectra. Small-scale field-aligned artificial irregularities (FAIs) were recognized from the
112 backscattered signals received at Hankasalmi, Finland (62.3° N; 26.6° E) by the CUTLASS (Co-
113 operative UK Twin Located Auroral Sounding System) HF coherent radar. The operation modes
114 of the UHF and CUTLASS radars and parameters estimated from their measurements are the
115 same as were used in Blagoveshchenskaya et al. (2014).

116 The observations of narrow band spectral components in the stimulated electromagnetic
117 emission (SEE) spectra were conducted on 21 October 2012 and 27 and 28 October 2013 in the
118 vicinity of St. Petersburg (60° N, 30° E) at a distance from Tromsø of about 1200 km. On 21
119 October 2012 the reception of HF heater signals was made with a Doppler spectral method in the
120 102 Hz band with a frequency resolution of 0.15 Hz. On 27 and 28 October 2013 the HF
121 receiving system, having a large dynamic range allowed the recording of signals in the frequency
122 band of ± 3 kHz around the HF pump frequency with a resolution of about 1 Hz. The double
123 rhombic HF antenna system oriented to Tromsø was utilized in all experiments for the narrow
124 band SEE observations. In the course of experiment on 21 October 2012 the high power HF
125 radio wave with alternating O/X-mode polarization was injected into the ionosphere at frequency
126 of 7.953 MHz by cycles of 10 min on, 5 min off at three positions of HF beam, 90° (vertical),
127 84° and 78° (magnetic field-aligned). Only for this experiment were the narrow band SEE
128 measurements near St. Petersburg accompanied by the “classic” stimulated electromagnetic
129 emission (SEE) observations at Tromsø in the frequency band of 200 kHz with a resolution of
130 200 Hz for searching the spectral component in the SEE spectra commonly observed under the

131 radiation of the O-polarized powerful HF radio waves. On 27 and 28 October 2013 HF pumping
132 was produced in the magnetic field - aligned direction at HF pump frequencies of 7.953 and 6.96
133 MHz respectively. The O/X-mode HF pumping was performed on 27 October 2013, when the
134 ratio of $f_H / foF2 \leq 1$, whereas only X-mode heating well above the critical frequency ($f_H / foF2$
135 > 1) was used on 28 October 2013.

136

137 **3. Observational results and discussion**

138

139 *3.1. HF-induced disturbances in the ionospheric plasma and small-scale field-aligned* 140 *irregularities*

141

142 Below we present experimental results related to the behavior of plasma parameters, HF-
143 induced turbulence and small-scale field-aligned artificial irregularities in the high latitude
144 ionospheric F2 layer induced by extraordinary polarized powerful HF radio waves injected into
145 the magnetic zenith at high heater frequencies ($f_H > 6.0$ MHz) depending on the ratio of the HF
146 pump frequency to O- and X-mode critical frequencies of the F2 layer. The distinctive feature of
147 the experiments discussed below is a wide range of critical frequency changes with the
148 unchanged pump frequency. It provides both a proper comparison of X-mode HF-induced
149 phenomena excited under different ratio of $f_H / foF2$ and an estimation of the frequency band
150 above the $foF2$ in which such X-mode phenomena are still possible.

151

152 *3.1.1. Experiment on 3 November 2013*

153 The HF pump wave was radiated at a heater frequency of 6.2 MHz parallel to the
154 magnetic field with an effective radiated power of about 450 MW, from 15.30 – 18 UT. In the
155 course of the experiment the critical frequencies $foF2$ gradually dropped from 6.7 MHz at 15.30
156 UT to 5.2 MHz at 18 UT. This makes possible the investigation of the X-mode HF-induced

157 effects depending on the ratio of heater frequency to the maximum plasma frequency from f_H
158 $/foF2 = 0.92$ to $f_H / foF2 = 1.2$ in the same experiment for the same background geophysical
159 situation. Figure 1 presents the EISCAT UHF radar observations from 15.30 – 18 UT. It shows
160 the altitude-temporal behavior of the electron density (N_e), electron temperature (T_e) and ion
161 velocities (V_i) as well as the N_e and T_e variations at fixed altitudes. From 15.30 to 17 UT the
162 heater frequencies were below or near critical frequency $foF2$ ($f_H / foF2 = 0.92 - 1.05$). In such
163 ionospheric conditions the O-mode effects can be excited and we have conducted the alternating
164 O/X pumping. From 17 UT, when the $foF2$ dropped to 5.8 MHz, only X-mode HF pumping was
165 performed.

166 O-mode heating produced strong electron temperature enhancements up to 2500 – 3000
167 K (see Fig. 1b and e). The electron heating was accompanied by the generation of upward ion
168 flows from the ionosphere above ~ 350 km (see Fig.1c), which has been observed in a large
169 number of previous EISCAT heating experiments from the UHF radar measurements (see, for a
170 example, Rietveld et al., 2003; Blagoveshchenskaya et al., 2005; Kosch et al., 2010; 2014). The
171 thermal electron heating produces the plasma pressure gradient leading the ions to move upward
172 along the magnetic field line (Kosch et al., 2010).

173 By contrast, an X-mode heating caused the strong apparent electron density
174 enhancements by 50-70% above the background N_e values, observed up to 600 km (see Fig.1a
175 and d). Such apparent N_e increases are a typical feature of X-mode heating at different heater
176 frequencies from EISCAT UHF radar observations (Blagoveshchenskaya et al., 2011a; 2013).
177 They can be accompanied by HF-enhanced ion and plasma lines (HFILs and HFPLs) in the UHF
178 radar spectra but not in all experiments. In the course of the experiment on 3 November 2013 not
179 too strong enhanced ion and plasma lines were observed in the first three X-mode pulses in the
180 altitude range of 220 -250 km, which did not allow the use of the standard analysis of the radar
181 spectra to get accurate N_e estimations. The N_e behavior at fixed heights (Fig. 1d) is given from
182 the altitude of 390 km, which is well above the altitude region occupied by HF-enhanced ion and

183 plasma lines. In the last three heater pulses HFILs and HFPLs were not excited at all and
184 therefore accurate estimations of the electron densities and temperatures can be performed in a
185 wide altitude range. However, the same Ne enhancements occurred even when the pump
186 frequency exceeded the $f_{x}F2$ from 17.30 UT ($f_H > f_{x}F2$). As was shown by Kuo et al. (2010), an
187 X-mode HF pump wave moves the ionospheric F-region upward. The origin of apparent strong
188 Ne enhancements observed under X-mode HF pumping at different heater frequencies is not yet
189 understood. In principle, the accelerated electrons could produce the enhanced ionization
190 Apparent Ne enhancements are typical for X-mode pumping and observed as often as the T_e
191 enhancements from UHF radar measurements under the action of O-polarized powerful HF radio
192 waves. Hence, an efficient mechanism of the electron acceleration in a wide altitude range
193 induced by an X-polarized pump wave should be found.

194 In the course of the X-mode pumping the apparent Ne enhancements were accompanied
195 by some T_e increases, which were weak (about 20 % above the background values) in two heater
196 pulses from 15.46 – 15.56 and 16.01 – 16.11 UT, when the heater frequency was below the
197 critical frequency f_oF2 . The T_e values, produced by ohmic heating, increased up to 50% after 17
198 UT, when f_H exceeded f_oF2 .

199 Small-scale field-aligned artificial irregularities (FAIs) with the spatial size across the
200 geomagnetic field of $l_{\perp} \approx 8 - 11.5$ m were observed throughout the experiment. This is seen in
201 Figure 2, in which CUTLASS (SuperDARN) Hankasalmi radar observations on 3 November
202 2013 are presented. Alternating O/X-mode heating was produced from 15.30 – 17 UT, when the
203 heater frequency was below and then near f_oF2 . Here the FAIs with scales of $l_{\perp} \approx 8 - 11.5$ m
204 were excited both for O- and X-mode HF pumping, but the intensity of the X-mode FAIs was
205 about 4 – 6 dB below that of the O-mode FAIs. This differs from effects observed at lower heater
206 frequencies ($f_H \leq 5.4$ MHz), when X-mode FAIs were not generated at all at heater frequencies
207 below f_oF2 (Robinson et al., 1997).

208 From 17 – 18 UT the critical frequency foF2 dropped from 5.9 to 5.2 MHz ($f_H / foF2 =$
209 1.05 – 1.19). In such conditions the O-mode effects are impossible and only X-mode HF
210 pumping was produced. As the foF2 values decreased, at first FAIs with $l_{\perp} \approx 8$ m, and thereafter
211 with $l_{\perp} \approx 9$ m disappeared (see Fig. 2). Small-scale irregularities with a transverse size of 11.5 m
212 were excited to 18 UT even when the f_H became above the $fxF2$ and an X-mode pump wave
213 cannot be longer reflected from the ionosphere. Moreover, their intensity, when $f_H / foF2 = 1.05$
214 – 1.19 was higher when compared with the case before 17 UT under $f_H / foF2 = 0.92 – 1.05$.

215

216 *3.1.2. Experiment on 28 October 2013*

217 The experiment was carried out from 15.30 – 18 UT when the critical frequency foF2
218 decreased over a wide range from 7.6 to 5.3 MHz. An X-polarized HF pump wave was radiated
219 at a heater frequency of 6.96 MHz along the magnetic field line with an effective radiated power
220 of about 550 MW. The distinctive feature of this X-mode experiment, as compared with the 3
221 November 2013 event, was the appearance of intense HF-enhanced ion and plasma lines in the
222 UHF radar spectra. Incoherent scatter radars are able to make direct measurements of
223 longitudinal plasma waves. The observed spectra under X-mode heating are typical signatures of
224 electrostatic plasma waves such as Langmuir and ion-acoustic waves. The conversion of
225 powerful electromagnetic HF wave to Langmuir and ion-acoustic waves is direct evidence for
226 the excitation of the parametric decay instability in the vicinity of the reflection height of the
227 pump wave (Fejer, 1979; Hagfors et al., 1983; DuBois et al., 1990; Stubbe et. al., 1992; Stubbe,
228 1996; Rietveld et al., 2000; Gurevich et al., 2004). The gradual decrease of foF2 over a wide
229 frequency range (7.6 – 5.3 MHz) with the use the a fixed heater frequency of $f_H = 6.96$ MHz
230 makes the detailed investigation of HF-enhanced ion and plasma lines (HFILs and HFPLs) under
231 different ratios of $f_H / foF2$ from 0.91 to 1.31 possible, permitting a clarification of the nature of
232 the observed phenomena and an estimation of the frequency band above foF2 in which such X-
233 mode phenomena are generated. The behavior of the undecoded downshifted plasma line power,

234 the altitude distribution of the plasma line intensity, the raw electron density, and the critical
235 frequency foF2 in the course of the experiment of 28 October 2013 are depicted in Figure 3. The
236 raw electron density is defined as the backscattered power of radar signal which points to the
237 generation of the ion lines in the radar spectra. As is evident from Fig.3, the intense HF-
238 enhanced plasma and ion lines were excited through the whole heater cycle on the interval
239 between 15.30 – 16.45 UT. At first the heater frequency was below or near foF2 ($f_H \leq foF2$) and
240 then lay in the frequency range between the ordinary and extraordinary mode critical frequency,
241 foF2 ($foF2 < f_H \leq fxF2$). An important point is that HF-induced plasma lines disappeared in the
242 first part of heater-on cycle from 16.46 – 16.56 UT where the heater frequency exceeded the
243 fxF2, $f_H > fxF2$ (see Fig.3 a, b). Remember, that $fxF2 = foF2 + f_{ce}/2 \approx (foF2 + 0.7)$ MHz, where
244 f_{ce} is the electron gyrofrequency. The disappearance of HFPLs was accompanied by a change in
245 the behavior of the backscattered power and therefore HF-enhanced ion lines (Fig. 3c), which
246 became much weaker and had a random character.

247 We also compared the behavior of ion and plasma line spectra for X-mode pumping
248 under different ratios of the heater frequency to the critical frequency of the F2 layer ($f_H / foF2 <$
249 1 and $f_H / foF2 > 1$). The procedure for obtaining the spectra is the same as described by
250 Blagoveshchenskaya et al. (2014). Figure 4 presents the maximum power of the HF-enhanced
251 downshifted plasma lines, upshifted and downshifted ion lines against altitude for HF pulses,
252 when $f_H / foF2 < 1$ (15.31 – 15.41 UT) and $f_H / foF2 > 1$ (16.31 – 16.41 UT) in the course of the
253 X-mode experiment on 28 October 2013. By and large they confirm the result presented by
254 Blagoveshchenskaya et al. (2014) for other EISCAT HF pumping experiments, when it was only
255 possible to make such a comparison between two heater pulses of different durations obtained
256 from two different experiments under different background conditions. As is obvious from Fig.
257 4, the altitude distribution of the downshifted ion line power exhibits two power maxima
258 observed both under $f_H / foF2 < 1$ (Fig. 4a) and $f_H / foF2 > 1$ (Fig. 4b). The HF-enhanced ion and

259 plasma lines were generated over a wider range of heights when $f_H / foF2 > 1$ as compared with
260 the event under $f_H / foF2 < 1$.

261 The CUTLASS Hankasalmi radar observations in the course of the X-mode experiment
262 on 28 October 2013 from 15.30 – 18 UT are presented in Figure 5. The CUTLASS radar ran at
263 operational frequencies of about 16, 18, and 20 MHz. Due to the Bragg condition ($l_{\perp} = c / 2f_R$,
264 where f_R is the radar operational frequency, and c is a speed of light) the size of FAIs
265 perpendicular to the magnetic field l_{\perp} responsible for the backscatter was about $l_{\perp} \approx 9, 8,$ and 7.5
266 m respectively. As is seen from Fig. 5, the artificial field-aligned irregularities were generated
267 throughout the experiment both when $f_H / foF2 < 1$ and $f_H / foF2 > 1$.

268 The artificial small-scale field-aligned irregularities were observed together with HF-
269 enhanced ion and plasma lines. However, FAIs with $l_{\perp} \approx 9$ and 8 m persisted to the present even
270 when HF-induced plasma lines disappeared. This occurred when f_H exceeded $fxF2$ and an X-
271 polarized pump wave can no longer be reflected from the ionosphere, whereas the larger scale of
272 FAIs in this experiment with $l_{\perp} \approx 9$, accompanied by apparent electron density enhancements,
273 were generated up to the end of experiment (18 UT), when the values of $foF2$ dropped to 5.3
274 MHz, showing that the heater frequency was above the $foF2$ by 1.7 MHz.

275 CUTLASS Hankasalmi radar measurements have demonstrated that at high heater
276 frequencies ($f_H > 6.0$ MHz) in the afternoon and evening hours the X-mode FAIs with size of $l_{\perp} \approx$
277 $7.5 - 11.5$ m were excited when the $f_H / foF2 < 1$ as well as $f_H / foF2 > 1$. Moreover, they can
278 even be excited under $f_H > fxF2$ up to 1 MHz. This differs from the X-mode FAIs at low heater
279 frequencies ($f_H \leq 5.4$ MHz), which cannot be generated, when heater frequencies lie below $foF2$.
280 However, such FAIs with $l_{\perp} \approx 11.5 - 15$ m were excited above the $foF2$ by $0.1 - 1.2$ MHz
281 (Blagoveshchenskaya et al. 2013). There is also a significant difference in the decay times for X-
282 mode FAIs excited at high and low heater frequencies. The FAI decay time at $f_H > 6.0$ MHz (see
283 Figs. 2 and 5) did not exceed 3 min in the evening hours whereas it can reach the unusually long
284 values of $15 - 20$ min at low heater frequencies between $3.95 - 5.423$ MHz (Blagoveshchenskaya

285 et al. 2011; 2013). In spite of the fact that the generation of FAIs induced by an X-polarized high
286 power HF radio wave is a repeatable and easily reproducible feature from EISCAT heating
287 experiments, the mechanism of their excitation is still remains poorly studied. Mention may be
288 made of the process of stimulated scattering of an X-mode powerful radio wave by ions with the
289 upper-hybrid or electron-cyclotron oscillations excited in the plasma (Vas'kov and Ryabova,
290 1998). Intense Langmuir waves can also generate FAI with a broad spectrum due to the
291 filamentation instability (Kuo and Schmidt, 1983). However, for the small-scale FAIs excited,
292 when high-power X-mode HF radio wave did not reflect from the ionosphere ($f_H > f_{XF2}$), the
293 most plausible mechanism for their generation could be closely related to and driven by the HF-
294 induced large-scale artificial irregularities. An X-polarized HF pump wave heats the F-region of
295 the ionosphere through collision processes more effectively as compared with the O-mode HF
296 pumping (Kuo et al., 2010). The artificial large-scale irregularities are formed at the heater
297 frequencies above and below the foF2 by the growth of a self-focusing instability of an HF pump
298 wave beam (Gurevich, 1978; Vas'kov and Gurevich, 1979).

299

300 3.2. *Magnetic zenith effect*

301

302 The magnetic zenith effect is a typical phenomenon observed in the high latitude
303 ionospheric plasma under the impact of high-power electromagnetic waves with ordinary
304 polarization (O-mode). The magnetic zenith effect comes from a nonlinear process of the
305 structuring HF waves along the magnetic field (Gurevich et al., 2002; 2005). Modification
306 experiments carried out at the EISCAT HF heater at Tromsø and HAARP at Gakona, Alaska,
307 have shown that the most intense HF-induced electron heating, optical emissions, and FAIs were
308 excited when the O-mode HF pump wave was transmitted in the magnetic field-aligned direction
309 (Kosch et al., 2002; Rietveld et al., 2003; Pedersen et al., 2003; Mishin et al., 2005). As was

310 shown by Isham et al. (1999), Langmuir wave intensities also maximized under HF pumping
311 parallel the magnetic field.

312 We have considered the EISCAT UHF radar observations in the course of the experiment
313 on 21 October 2012. The experiment was carried out from 14 -16 UT under quiet magnetic
314 conditions, when the critical frequency of the F2 layer gradually dropped from 8.9 MHz at 14
315 UT to 7.6 MHz at 16 UT. High power HF radio waves were injected into the ionosphere at a
316 frequency of 7.953 MHz in cycles of 10 min on, 5 min off at three positions of the HF beam, 90°
317 (vertical), 84° and 78° (magnetic field-aligned). From cycle to cycle the polarization of HF pump
318 wave was changed between O- and X-mode. The effective radiated power was about ERP = 650
319 MW. In the course of each HF pulse the elevation angle of the UHF radar was changed every
320 minute from 74 to 90°. The X-mode pulses have demonstrated that the most intense HF-
321 enhanced ion and plasma lines (HFILs and HFPLs) from the incoherent scatter radar
322 observations, which are direct evidence of the parametric decay instability, were observed when
323 the high-power HF electromagnetic wave was injected towards the magnetic zenith (77°). For X-
324 mode injections in the vertical direction (90°), the HFILs and HFPLs were not excited. When the
325 HF pump wave was radiated in the 84° direction, HF-enhanced ion and plasma lines were much
326 weaker as compared with the 77° pointing direction. The same is true for the apparent electron
327 density and temperature enhancements observed from the EISCAT UHF radar observations. An
328 O-mode HF pumping shows the appearance of HFILs and HFPLs under any incidence angle of
329 the HF pump wave (90, 84 and 77°). The intensities of the HFILs and HFPLs for O- mode
330 pumping maximized for HF pumping towards the magnetic zenith, that is in agreement with
331 previous O-mode observations (Isham et al., 1999). However, their intensity was much weaker
332 as compared with the X-mode HFILs and HFPLs.

333 Further to this, we consider the behavior of HF-enhanced ion and plasma lines depending
334 on the elevation angle of the EISCAT UHF radar, when the heater frequency is above the critical
335 frequency of the F2 layer. The experiment was carried out on 2 November 2013 in the evening

336 hours. The HF pump wave with X-polarization was transmitted at a frequency of 6.96 MHz
337 towards the magnetic zenith. The effective radiated power was about 550 MW. During each 20
338 min heater pulse the elevation angle of the EISCAT UHF radar was changed between 72 and
339 86°. As an example, Figure 6 depicts the intensities of the undecoded downshifted plasma lines
340 and raw electron density (backscattered power) from 14.30 – 15 UT. During this pulse the heater
341 frequency of $f_H = 6.96$ MHz exceeded the critical frequency of $f_{oF2} = 6.4$ MHz ($f_H / f_{oF2} =$
342 1.09). It is seen that HF-enhanced ion and plasma lines were excited for radar elevation angles
343 between 76 - 79°, being the most intense in the field-aligned pointing the UHF radar (77°).

344 The ion line spectra obtained from the EISCAT UHF radar measurements for different
345 radar elevation angles of 76, 77, 78, and 79° are shown in Figure 7. The following features of the
346 ion line spectra in the magnetic field-aligned direction, when the heater frequency exceeded the
347 f_{oF2} , can be seen from Fig. 7: (1) intensities of the upshifted and downshifted ion lines are
348 maximized; (2) the appearance of two power maxima at different altitudes is observed both for
349 downshifted and upshifted ion lines; (3) the appearance of a nonshifted (zero frequency) spectral
350 component.

351 As is evident from the EISCAT UHF radar spectra, an X-mode HF heater wave
352 transmitted parallel to the magnetic field at heater frequencies above the critical frequency f_{oF2}
353 is able to excite intense HF-enhanced ion lines (upshifted, downshifted and nonshifted) and
354 plasma lines. The most intense HF-enhanced ion and plasma lines were generated when the
355 position of the HF heater beam and UHF radar were field-aligned, therefore, they exhibit a
356 strong magnetic zenith effect similar to the O-mode heating at frequencies below the f_{oF2} , as
357 was shown by Isham et al. (1999). Such HF-enhanced ion and plasma lines are indicative of the
358 parametric decay instability (PDI) and oscillating two stream instability (OTSI) (Fejer, 1979;
359 Dysthe et al., 1983; Stubbe, 1996, Kuo et al., 1997). PDI and OTSI give the most effective
360 channels to convert electromagnetic HF radio waves to electrostatic plasma waves, including
361 Langmuir waves of high frequency and ion acoustic waves of low frequency. In spite of HF-

362 enhanced ion and plasma lines (HFPLs and HFILs) in the incoherent radar spectra being
363 indicative of the parametric decay instability, it is still not clear in what way an X-mode pump
364 wave can excite the PDI and even OTSI, especially taking into account that the X-mode HFPLs
365 and HFILs were much higher intensity, as compared with the O-mode effects, and were observed
366 through the whole HF heater cycle together with artificial small-scale field-aligned irregularities
367 (Blagoveshchenskaya et al., 2014).

368

369 3.3 *Stimulated electromagnetic emissions*

370

371 The stimulated electromagnetic emission (SEE) was discovered by Thidé et al. (1982) at
372 the HF heating facility near Tromsø (Norway). During the last three decades the classical SEE
373 spectral components with an offset of 1 kHz up to 200 kHz from the HF heater frequency have
374 been extensively studied at different HF heating facilities located at mid- and high latitudes (see,
375 for example, Leyser, 2001 and references therein). The most common SEE spectral feature,
376 observed when the O-polarized HF pump wave is radiated in the vicinity of the vertical direction
377 at a frequency below the critical frequency f_oF2 and away from the electron gyro harmonic
378 frequency, is the downshifted maximum (DM). The DM is a strong emission with a pronounced
379 peak downshifted by 8 - 12 kHz below the heater frequency f_H (Thidé et al., 1982).

380 Recent experiments at the HAARP facility in Gakona, Alaska, have demonstrated the
381 generation of narrow band SEE spectral components within 1 kHz of the HF pump frequency,
382 produced by the stimulated Brillouin scatter (SBS) (Norin et al., 2009; Bernhardt, et al., 2009;
383 2010; Fu et al., 2013). Such strong components are shifted only by tens of Hz from the HF pump
384 frequency. Their origin is explained by the parametric decay of an ordinary (O-mode) polarized
385 powerful HF electromagnetic wave to the electrostatic (ion acoustic or ion cyclotron) wave with
386 the secondary electromagnetic wave scattered by SBS (Dysthe et al., 1977; Fejer, 1977; Norin et
387 al., 2009; Bernhardt, et al., 2010; Fu et al., 2013; Mahmoudian et al., 2013). The ion acoustic

388 (IA) spectral component appears with a frequency offset of 10 - 30 Hz (Bernhardt et al., 2009)
389 and the electrostatic ion cyclotron (EIC) line with frequency offset about of 50 Hz (for O⁺ ions)
390 from the HF pump frequency (Bernhardt et al., 2010; Mahmoudian et al., 2013). Observations of
391 the narrow band spectral components at the second harmonic of the electron cyclotron frequency
392 showed the excitation of harmonic sidebands near multiples of the ion cyclotron frequency
393 produced by the stimulated ion Bernstein emissions (Bernhardt et al., 2011). It is important to
394 mention that the variety of the narrow band spectral components in the SEE spectra, such as the
395 ion acoustic, electrostatic ion cyclotron and ion Bernstein waves, were observed in the vicinity of
396 the HAARP facility only for O-mode pumping of the ionosphere.

397 Below we present the first experimental evidence of the generation of the various narrow
398 band spectral components in the SEE spectra in the F region of the high latitude ionosphere
399 induced by an extraordinary (X-mode) powerful HF radio wave and recorded far away from the
400 HF heating facility. The first observations of the narrow band spectral component within 100 Hz
401 band frequency under X-mode pumping, was made on 21 October 2012 near St. Petersburg at a
402 distance of 1200 km away from the HF heater. These observations were accompanied by
403 EISCAT UHF radar measurements and “classic” SEE measurements in the 200 kHz band at
404 Tromsø. Observational results showing the spectrogram of the heater signal within a 100 Hz
405 frequency band are depicted in Figure 8 (top panel). For comparison, the “classic” SEE dynamic
406 spectra (spectrograms) recorded at Tromsø are presented in Fig. 8 (bottom panel). Details of the
407 experiment on 21 October 2012 and the behaviors of the HF-enhanced ion and plasma lines
408 (HFILs and HFPLs) from UHF radar observations are given in Section 3.2.

409 An unexpected feature was found in the spectra within 100 Hz of the HF heater frequency
410 received near St. Petersburg at a distance of 1200 km from the EISCAT HF heater facility (Fig.
411 8, top panel). During X-mode pulses with the HF beam pointing in the magnetic field-aligned
412 direction (14.46 -14.56 and 15.46 – 15.56 UT), a defined spectral component downshifted by 26
413 - 37 Hz below the heater frequency can be seen. Such a spectral component was not recognized

414 under vertical pointing the HF beam and was very weak, when X-mode HF pumping was
415 produced at an elevation angle of 84° (15.16 – 15.26 UT). It is an indication of the magnetic
416 zenith effect in the X-mode narrow band spectral component behavior. There is a close
417 correlation between the narrow band spectral lines and the HF-enhanced ion lines (HFILs) from
418 the EISCAT UHF radar observations. As was mentioned in Section 2.2, the strongest HFILs
419 were observed under X-mode pumping towards the magnetic zenith. They were much weaker in
420 the 84° direction and were not excited at all for X-mode injections in vertical direction (90°). We
421 suggest that the spectral component with the frequency offset 26 - 37 Hz observed under X-mode
422 HF pumping towards the magnetic zenith can be attributed to the stimulated Brillouin scatter
423 process in which the excited electrostatic wave could be an ion acoustic wave. The O-mode
424 pumping cycles at any position of HF heater beam did not show the presence of defined spectral
425 components within 100 Hz at a distance far away from the HF heater, in spite of the generation
426 of HFILs under any incidence angle of the HF pump wave.

427 Unfortunately, we were not able to carry out the narrow band SEE measurements at
428 Tromsø in the vicinity of the HF heating facility. The frequency resolution of the SEE equipment
429 used (200 Hz) was not sufficient to observe the narrow band SEE. As a consequence only the
430 “classic” SEE measurements at the frequency band of 200 kHz were conducted. As is seen, SEE
431 observations near Tromsø (Fig. 8, bottom panel) show the appearance of a well-defined DM
432 component in the SEE spectra downshifted by about 12 kHz from the heater frequency and
433 observed only during O-mode heater pulses in any position of the HF heater beam (90° , 84° , 78°).
434 The X-mode pulses did not exhibit any defined spectral components offset from one to tens kHz
435 from the heater frequency, but the X-mode SEE spectra were very noisy as compared with the O-
436 mode spectra. The generation of a DM component for O-mode pumping was accompanied by
437 strong small-scale artificial field-aligned irregularities (FAIs). In such conditions X-mode FAIs
438 were also excited but their intensity was weaker as compared with O-mode FAIs.

439 In subsequent experiments on 27 and 28 October 2013, the HF receiving system, which
440 allowed the recording of the heater signals in the frequency band of ± 3 kHz around the HF pump
441 frequency with a resolution of about 1 Hz, was used for observations near St. Petersburg. On 27
442 October 2013 narrow band SEE observations were conducted from 12 to 13.30 UT under quiet
443 magnetic conditions, when the critical frequency of the F2 layer slightly dropped from 10.4 to
444 9.4 MHz. An HF pump wave with O/X polarization was radiated at frequency of 7.953 MHz
445 towards the magnetic zenith by cycles of 20 min on, 10 min off. The effective radiated power
446 was about ERP = 650 MW. The spectrogram of the heater signal within 600 Hz recorded near St.
447 Petersburg on 27 October 2013 is shown in Figure 9a. As is seen, the O-mode pulse from 12.01 –
448 12.21 UT, similarly to the O-mode cycles on 21 October 2012, did not exhibit any narrow band
449 spectral components at distance far away from HF heater. By contrast, the subsequent two X-
450 mode cycles (12.31 – 12.51 and 13.01 – 13.21 UT) under the same background conditions have
451 demonstrated a variety of well defined narrow band spectral lines below and above the pump
452 frequency. Figure 9b depicts the power spectra obtained at different times in the course of the X-
453 mode pulse from 12.31 – 12.51 UT. The spectra show the well-defined narrow band spectral lines
454 downshifted and upshifted by about 55 Hz from the pump frequency, which can be attributed to
455 the electrostatic ion cyclotron (EIC) waves, and their multiple harmonics (up to four discrete
456 spectral lines). The downshifted emissions were paired with upshifted spectral components. The
457 intensity of the main downshifted emission was below the HF pump wave by – (20-30) dB
458 during the pump pulse from 12.31 – 12.51 UT. It is important, that for the conditions of this
459 experiment the HF pump frequency was near the sixth electron gyro harmonic frequency (below
460 by about 200 kHz). The observed multiple spectral lines are similar to structures ordered by
461 harmonics of the ion gyro frequency observed in the vicinity of the HAARP heating facility in
462 the course of O-mode HF pumping experiment near the second electron gyro harmonic
463 frequency, and are caused by stimulated ion Bernstein emissions (Bernhardt et al., 2011).

464 Coincident with the electrostatic ion cyclotron harmonic waves, the spectral lines
465 downshifted by 28 and 84 Hz can be recognized in Fig. 9b. They can be attributed to the first and
466 third harmonic of an ion acoustic wave. The second harmonic (56 Hz) cannot be resolved due to
467 the strong EIC wave downshifted by about 55 Hz from the pump frequency with a width of the
468 order of 10 Hz. In the course of the HF pump pulses the HF-enhanced ion lines and FAIs were
469 excited. Their behavior for O- and X-mode pulses is very similar to those previously described
470 for the experiment on 21 October 2012.

471 On 28 October 2013 narrow band SEE observations near St. Petersburg were carried out
472 from 17 – 18 UT. The distinctive feature of the experiment is that the measurements were made
473 when the heater frequency exceeded foF2 as well as fxF2. The critical frequency foF2 dropped
474 from 5.8 MHz at 17 UT to 5.3 at 18 UT, while the X-polarized HF pump wave was at 6.96 MHz.
475 The details of HF pumping and experimental results from EISCAT UHF radar and CUTLSS
476 observations on 28 October 2013 from 15.30 – 18 UT are given in Section 3.1.2. SEE
477 observations were conducted only in the last hour of this experiment.

478 Figure 10a demonstrates the spectrogram of the heater signal within 400 Hz recorded
479 near St. Petersburg on 28 October 2013 from 17 to 18 UT. As is seen, the only very intense
480 spectral line downshifted by about 55 Hz from the HF pump frequency was recorded in all X-
481 mode heater pulses. As an example, Figure 10b shows the power spectra of the pump wave
482 obtained at different times of the heating cycle from 17.01 – 17.11 UT. The observed emission
483 line can be attributed to the electrostatic ion cyclotron wave. The intensity of this spectral
484 emission was only 5 -15 dB less than the HF pump wave intensity. As was shown in Section
485 3.1.2, at pump frequencies lying above the extraordinary critical frequency fxF2, HF-enhanced
486 ion and plasma lines are not excited. However, even when $f_H > f_{xF2}$, some sporadic burst-like
487 HFILs can be seen from UHF radar observations (see Fig. 3). The X-mode FAIs were generated
488 up to 18 UT (see Fig. 5).

489 The observations of the narrow band SEE spectral components under X-mode HF
490 pumping demonstrate evidence of the excitation of various narrow band spectral components in
491 the SEE spectra (within 1 kHz of the pump frequency), which can be associated with the ion
492 acoustic (IA), electrostatic ion cyclotron (EIC), and electrostatic ion cyclotron harmonic waves
493 (otherwise known as neutralized ion Bernstein waves). It has been suggested that these spectral
494 components can be attributed to the stimulated Brillouin scatter (SBS) process. The results
495 obtained have shown that an X-polarized electromagnetic wave scattered by SBS can propagate
496 more than one thousand km without significant deterioration. It is important to note that O-mode
497 narrow band spectral lines were not observed at a large distance from the EISCAT HF heating
498 facility.

499

500 **4. Summary and concluding remarks**

501

502 We have presented experimental results related to the variety of phenomena in the high
503 latitude ionospheric F2 layer induced by an extraordinary (X-mode) HF pump wave at high
504 heater frequencies ($f_H = 6.2 - 8.0$ MHz) depending on the pump proximity to the critical
505 frequencies f_oF2 and f_xF2 . Results come from a large body of X-mode HF pumping experiments
506 at the EISCAT HF heating facility in October 2012 and October – November 2013 with the use
507 of multi-instrument diagnostics. X-mode HF pumping experiments have been carried out at high
508 heater frequencies of 6.2, 6.96, and 7.953 MHz in quiet magnetic conditions under effective
509 radiated powers of 450 – 650 MW. The distinctive feature of the experiments is a wide diapason
510 of critical frequency changes, when the f_H / f_oF2 ratio was varied through a range from 0.9 to
511 1.35. It provides both a proper comparison of X-mode HF-induced phenomena excited under
512 different ratio of f_H / f_oF2 and an estimation of the frequency band above the f_oF2 in which such
513 X-mode phenomena are still possible.

514 Intense HF-enhanced ion and plasma lines (HFILs and HFPLs) in the UHF radar spectra,
515 which are the typical signatures of ion-acoustic and Langmuir waves, were excited through the
516 HF pump pulse under different ratios of heater frequency to the maximum plasma frequency ($f_H /$
517 $f_{oF2} \leq 1$ and $f_H / f_{oF2} > 1$). The generation of the HFILs and HFPLs above f_{oF2} occurred in the
518 frequency range between the ordinary and extraordinary mode critical frequencies, $f_{oF2} \leq f_H \leq$
519 f_{xF2} . An important point is that HF-induced plasma and ion lines disappeared when the heater
520 frequency exceeded the f_{xF2} and an X-polarized pump wave can no longer be reflected from the
521 ionosphere.

522 HF-enhanced ion and plasma lines were accompanied by the generation of small-scale
523 artificial field-aligned irregularities (FAIs) with a spatial size across the geomagnetic field of $l_{\perp} \approx$
524 7.5 – 9 m. An unexpected feature in the FAI behavior is their generation under conditions when
525 the X-mode wave cannot be reflected from the ionosphere (f_H exceeded f_{xF2}) and HF-enhanced
526 plasma and ion lines were not excited. Under such conditions FAIs were accompanied by
527 apparent electron density enhancements and the electron heating increased by 50% from the
528 background values. In spite of the fact that the generation of X-mode FAIs is a repeatable feature
529 from EISCAT heating experiments, the mechanism of their excitation remains poorly studied.
530 Mention may be made of the process of stimulated scattering an X-mode powerful radio wave by
531 ions (Vas'kov and Ryabova, 1998) and intense Langmuir waves which can also generate FAI
532 with a broad spectrum due to the filamentation instability (Kuo and Schmidt, 1983). However,
533 for the FAIs excited under $f_H > f_{xF2}$, the most plausible mechanism of their generation could be
534 closely related to and driven by HF-induced large-scale artificial irregularities.

535 The magnetic zenith effect was found in the behavior of the X-mode HF-enhanced ion
536 and plasma lines. X-mode pumping experiments under different pointing directions of the HF
537 antenna beam (90, 84 and 77°) have demonstrated that the most intense HF-enhanced ion and
538 plasma lines were observed when the high-power HF electromagnetic wave was transmitted
539 towards the magnetic zenith (77°). Experimental results from an elevation angle stepping of the

540 EISCAT UHF radar between 72 and 90° have also shown that at heater frequencies above the
541 critical frequency foF2 the most intense HF-enhanced ion (upshifted, downshifted and
542 nonshifted) and plasma lines were generated when the UHF radar was pointing field-aligned.
543 Such HF-enhanced ion and plasma lines are indicative of the parametric decay instability (PDI)
544 and oscillating two stream instability (OTSI) excited above foF2. The same is true for the
545 apparent electron density enhancements observed from the EISCAT UHF radar observations.

546 We have presented the first experimental evidence showing that an extraordinary (X-
547 mode) powerful HF radio wave is able to generate different narrow band spectral components in
548 the SEE spectra (within 1 kHz of pump frequency) in the F region of the high latitude
549 ionosphere, which were recorded far away from the HF heating facility. The observed X-mode
550 spectral lines can be associated with the ion acoustic (IA), electrostatic ion cyclotron (EIC), and
551 electrostatic ion cyclotron harmonic waves (otherwise known as neutralized ion Bernstein
552 waves). It has been suggested that these spectral components can be attributed to the stimulated
553 Brillouin scatter (SBS) process in which the excited electrostatic wave could be an ion acoustic or
554 electrostatic ion cyclotron waves. Similar narrow band SEE spectral lines, induced by the
555 ordinary (O-mode) polarized HF pump wave, were observed in the HAARP experiments in the
556 immediate vicinity (by 20 km) of the HF heating facility (Bernhardt, et al., 2009; 2010; 2011; Fu
557 et al., 2013). However, the comparison between the O- and X-mode narrow band spectra within
558 1 kHz from the pump frequency clearly demonstrated that only an X-polarized electromagnetic
559 wave scattered by SBS can propagate more than one thousand km without significant
560 deterioration. O-mode narrow band spectral lines were not observed at a large distance from the
561 EISCAT HF heating facility.

562 In spite of the fact that excitation of intense X-mode HF-induced phenomena in the F-
563 region of the high latitude ionosphere is a repeatable and easily reproducible feature from
564 EISCAT heating experiments, many aspects of the nonlinear interaction between an X-polarized
565 HF pump wave and the ionosphere plasma are still remain poorly understood and require further

566 theoretical as well as experimental research. Among the theoretical aspects we would like to
567 point out the following.

568 HF-enhanced ion and plasma lines in the incoherent radar spectra are indicative of the
569 parametric decay instability, but it is not clear through what mechanism an X-mode pump wave
570 can excite the PDI and even OTSI, especially taking into account that the X-mode HF-induced
571 ion and plasma lines are much higher intensity, as compared with the O-mode effects, are
572 observed through the whole HF pump pulse and coexist with strong artificial small-scale field-
573 aligned irregularities.

574 The generation mechanisms of small-scale artificial field-aligned irregularities needs
575 validation, particularly for FAIs excited when the heater frequency exceeds the f_{XF2} and an X-
576 polarized pump wave cannot be reflected from the ionosphere.

577 Strong apparent Ne enhancements from EISCAT UHF radar measurements are typical for
578 X-mode pumping and are observed as often as the Te enhancements under the action of O-
579 polarized HF pump waves. They occurred along the magnetic field line in a wide altitude range
580 whether the HF-enhanced ion and plasma lines were excited or not. The origin of such apparent
581 Ne enhancements under X-mode HF pumping at different heater frequencies is not yet
582 understood and needs the clarification. In principle, the accelerated electrons can produce the
583 enhanced ionization. Hence, an efficient mechanism of the electron acceleration induced by an
584 X-polarized pump wave should be found.

585 In closing, we list desirable experiments to be carried out in future for better
586 understanding the unusually strong phenomena in the F-region of the ionosphere induced by an
587 X-polarized HF pump wave. It is known that significant changes of phenomena, excited near the
588 upper hybrid resonance altitude and the reflection height of the ordinary (O-mode) HF pump
589 wave, occur when the HF pump frequency is lying in the vicinity of the electron gyro harmonic
590 frequency. HF-induced effects in the vicinity of the electron gyro harmonics have been
591 extensively studied at different HF heating facilities. It will be interesting to investigate the

592 electron gyro harmonic effects under an X-mode HF pumping into the F-region of the
593 ionosphere for different numbers of electron gyroharmonics. There is also a need to find out the
594 influence of the HF heater beam width and effective radiated power on characteristics of the
595 plasma turbulence and other phenomena associated with the X-mode plasma modification. It is
596 important to determine the threshold values of effective radiated power (ERP) needed to generate
597 various X-mode HF-induced phenomena at heater frequencies f_H lying above and below the
598 critical frequency f_oF2 as well as to compare the ERP thresholds of alternating O/X-mode
599 effects at heater frequencies $f_H \leq f_oF2$. It is of interest also to compare the simultaneous
600 observations of the narrow band spectral emissions in the immediate vicinity of HF heating
601 facility and far away from it for O- and X-mode HF pumping of the high latitude ionospheric F
602 region. Such narrow band SEE observations should be accompanied by UHF incoherent scatter
603 radar and HF coherent scatter radar measurements.

604

605 **Acknowledgements.** EISCAT is an international scientific association supported by research
606 organizations in China (CRIRP), Finland (SA), Japan (NIPR and STEL), Norway (NFR),
607 Sweden (VR), and the United Kingdom (NERC). CUTLASS is supported by the Finnish
608 Meteorological Institute, and the Swedish Institute of Space Physics. TKY is supported by
609 NERC grant NE/K011766/1. We thank Dr. M. Rietveld for help with EISCAT HF pumping
610 experiments and SEE data from Tromsø site.

611

612 **References**

613

- 614 Bernhardt, P.A., Selcher, C.A., Lehmberg, R.H., Rodriguez, S.P., Thomason, J.F., McCarrick,
615 M.J., Frazer, G.J., 2009. Determination of the electron temperature in the modified
616 ionosphere over HAARP using the HF pumped Stimulated Brillouin Scatter (SBS) emission
617 lines. *Annales Geophysicae* 27, 4409-4427.
- 618 Bernhardt, P. A., Selcher, C.A., Lehmberg, R.H., Rodriguez, S.P., Thomason, J.F., Groves,
619 K.M., McCarrick, M.J., Frazer, G.J., 2010. Stimulated Brillouin Scatter in a magnetized
620 ionospheric plasma. *Physics Review Letters* 104, 165004,
621 doi:10.1103/PhysRevLett.104.165004.
- 622 Bernhardt, P.A., Selcher, C. A., Kowtha, S., 2011. Electron and ion Bernstein waves excited in
623 the ionosphere by high power EM waves at the second harmonic of the electron cyclotron
624 frequency, 2011. *Geophysical Research Letters*, 38, doi:10.1029/2011GL049390.
- 625 Blagoveshchenskaya, N. F., Kornienko, V.A., Borisova, T.D., Rietveld, M.T., Böisinger, T.,
626 Thidé, B., Leyser, T.B., Brekke, A., 2005. Heater-induced phenomena in a coupled
627 ionosphere-magnetosphere system. *Advances in Space Research* 38, 2495–2502.
- 628 Blagoveshchenskaya, N. F., Borisova, T. D., Yeoman, T., Rietveld, M. T., Ivanova, I.M.,
629 Baddeley, L.J., 2011a. Artificial field-aligned irregularities in the high-latitude F region of
630 the ionosphere induced by an X-mode HF heater wave. *Geophysical Research Letters* 38,
631 doi: 10.1029/2011GL046724.
- 632 Blagoveshchenskaya, N. F., Borisova, T.D., Yeoman, T. K., Rietveld, M. T., 2011b. The effects
633 of modification of a high-latitude ionosphere by high-power HF radio waves. Part 1. Results
634 of multi-instrument ground-based observations. *Radiophysics and Quantum Electronics*
635 (Engl. Transl.) 53, (9–10), 512 – 531.
- 636 Blagoveshchenskaya, N. F., Borisova, T. D., Yeoman, T. K., Rietveld, M. T., Häggström, I.,
637 Ivanova, I. M., 2013. Plasma modifications induced by an X-mode HF heater wave in the

638 high latitude F region of the ionosphere. *Journal of Atmospheric and Solar-Terrestrial*
639 *Physics* 105-106, 231 – 244.

640 Blagoveshchenskaya, N. F., Borisova, T. D., Kosch, M., Sergienko, T., Brändström, U.,
641 Yeoman, T. K., Häggström I., 2014. Optical and Ionospheric Phenomena at EISCAT under
642 Continuous X-mode HF Pumping. *Journal of Geophysical Research: Space Physics* 119,
643 10,483–10,498, doi:10.1002/2014JA020658.

644 DuBois, D. F., Rose, H. A., Russell, D., 1990. Excitation of strong Langmuir turbulence in
645 plasmas near critical density: Application to HF heating of the ionosphere. *Journal of*
646 *Geophysical Research* 95, 21221–21272.

647 Dunkan, L.M., Behnke, R.A., 1978. Observations of self-focusing electromagnetic waves in the
648 ionosphere. *Physics Review Letters* 41, 998 – 1001.

649 Dysthe, K.B., Leer, E., Trulsen, J., Stenflo, L., 1977. Stimulated Brillouin scattering in the
650 ionosphere. *Journal of Geophysical Research* 82, 717 – 718.

651 Dysthe, K.B., Mjølhus, E., Pécseli, H.L., Rypdal, K., 1983. A thermal oscillating two-stream
652 instability. *Physics Fluids* 26, 146 – 157.

653 Erukhimov, L.M., Metelev, S.A., Myasnikov, E.N., Mityakov, N.A., Frolov, V.L., 1987.
654 Artificial ionospheric turbulence (review). *Radiophysics and Quantum Electronics (Engl.*
655 *Transl.)* 31, 156 – 171.

656 Farley, D.T., LaHoz, C., Fejer, B.G., 1983. Studies of the self-focusing instability at Arecibo.
657 *Journal of Geophysical Research* 88, 2093 – 2102.

658 Fejer, J.A., 1977. Stimulated Brillouin scattering and incoherent backscatter. *Geophysical*
659 *Research Letters* 4, 289 – 290.

660 Fejer, J.A., 1979. Ionospheric Modification and Parametric Instabilities. *Rev. Geophys. Space*
661 *Phys.*, 17 (1), 135 - 153.

662 Frolov, V.L., Bolotin, I.A., Komrakov, G.P., et al., 2014. Generation of artificial ionospheric
663 irregularities in the midlatitude ionosphere modified by high-power high-frequency X-mode

664 radio waves. *Radiophysics and Quantum Electronics (Engl. Transl.)* 57, (6), 393 – 416.

665 Fu, H., Scales, W. A., Bernhardt, P. A., Samimi, A., Mahmoudian, A., Briczinski, S. J.,
666 McCarrick, M. J., 2013. Stimulated Brillouin scatter and stimulated ion Bernstein scatter
667 during electron gyroharmonic heating experiments. *Radio Science* 48, 607-616,
668 doi:10.1002/2013RS005262.

669 Gurevich, A. V., 1978. *Nonlinear Phenomena in the Ionosphere*. Springer-Verlag, New York.

670 Gurevich, A., Zybin, K. Carlson, H., Pedersen, T., 2002. Magnetic zenith effect in ionospheric
671 modifications. *Physics Letters A* 305, (5), 264–274.

672 Gurevich, A.V., Carlson, H.C., Medvedev, Yu.V., Zybin, K.R., 2004. Langmuir turbulence in
673 ionospheric plasma, *Plasma Physics Reports*, 30, 995–1005.

674 Gurevich, A., Zybin, K. Carlson, H., 2005. Magnetic zenith effect in ionospheric modifications.
675 *Radiophysics and Quantum Electronics (Engl. Transl.)* 48, (9), 686 – 699.

676 Gurevich, A.V., 2007. Nonlinear effects in the ionosphere. *Physics – Uspekhi (Engl. Transl.)* 50,
677 1091 – 1121.

678 Hagfors, T., Kofman, W., Kopka, H., Stubbe, P., Ijnen, T., 1983. Observations of enhanced
679 plasma lines by EISCAT during heating experiments. *Radio Science* 18, 861 – 866.

680 Isham, B., Rietveld, M., Hagfors, T., LaHoz, C., Mishin, E., Kofman, W., Leyser, T., van Eyken,
681 A., 1990. Aspect angle dependence of HF enhanced incoherent backscatter. *Advances in*
682 *Space Research* 24, (8), 1003–1006.

683 Kosch, M., Rietveld, M., Yeoman, T., Cierpka, K., Hagfors, T., 2002. The high-latitude artificial
684 aurora of 21 February 1999: An analysis. *Advances in Polar Upper Atmosphere Research* 16,
685 1–12.

686 Kosch, M. J., Ogawa, Y., Rietveld, M.T., Nozawa, S., Fujii, R., 2010. An analysis of pump-
687 induced artificial ionospheric ion upwelling at EISCAT. *Journal of Geophysical Research*
688 115, A12317, doi:10.1029/2010JA015854.

689 Kosch, M. J., Vickers, H., Ogawa, Y., Senior, A., Blagoveshchenskaya, N., 2014. First

690 observation of the anomalous electric field in the topside ionosphere by ionospheric
691 modification over EISCAT. *Geophysical Research Letters* 41, doi:10.1002/ 2014GL061679.

692 Kuo, S.P., Schmidt, G, 1983. Filamentation instability in magneto plasmas. *Physics Fluids* 26,
693 2529 – 2536.

694 Kuo, S., Lee, M., Kossey, P.,1997. Excitation of oscillating two stream instability by upper
695 hybrid pump in ionospheric heating experiments at Tromsø. *Geophysical Research Letters*
696 24, 2969 -2972.

697 Kuo, S., Cheng, W.-T., Snyder, A., Kossey, P., Battis, J., 2010. Contrasting O/X-mode heater
698 effects on O-mode sounding echo and the generation of magnetic pulsations. *Geophysical*
699 *Research Letters* 37, L01101, doi: 10.1029/2009GL041471.

700 Leyser, T. B., 2001. Stimulated electromagnetic emissions by high-frequency electromagnetic
701 pumping of the ionospheric plasma. *Space Science Review* 98, 223 – 328.

702 Lofas, H., Ivchenko, N., Gustavsson, B., Leyser, T.B., Rietveld, M.T., 2009. F-region electron
703 heating by X-mode radiowaves in underdense conditions. *Annales Geophysicae* 27, 2585 –
704 2592.

705 Mahmoudian, A., Scales, W. A., Bernhardt, P. A., Fu, H., Briczinski, S. J., McCarrick M. J.,
706 2013. Investigation of ionospheric stimulated Brillouin scatter generated at pump frequencies
707 near electron gyroharmonics. *Radio Science* 48, 685697, doi:10.1002/2013RS005189.

708 Mishin, E.V., Burke, W. J., Pedersen, T., 2005. HF-induced airglow at magnetic zenith:
709 theoretical considerations. *Annales Geophysicae* 23, 47 – 53.

710 Norin, L., Leyser, T. B., Nordblad, E., Thidé, B., and McCarrick, M., 2009. Unprecedentedly
711 strong and narrow electromagnetic emissions stimulated by high-frequency radio waves in
712 the ionosphere. *Physics Review Letters* 102, 065003, doi:PhysRevLett102.065003..

713 Pedersen, T. R., McCarrick, M., Gerken, E., Selcher, C., Sentman, D., Carlson, H. C., Gurevich,
714 A., 2003. Magnetic zenith enhancement of HF radio-induced airglow production at HAARP,
715 *Geophysical Research Letters* 30, (A4), 1169, doi:10.1029/2002GL016096.

716 Rietveld, M.T., Isham, B., Kohl, H., Hoz, C.L., Hagfors, T., 2000. Measurements of HF-
717 enhanced plasma and ion lines at EISCAT with high altitude resolution. *Journal of*
718 *Geophysical Research* 105, 7429 – 7439.

719 Rietveld, M.T., Kosch, M. J., Blagoveshchenskaya, N.F., Kornienko, V.A., Leyser, T.B.,
720 Yeoman, T.K., 2003. Ionospheric electron heating, aurora and striations induced by powerful
721 HF radio waves at high latitudes: aspect angle dependence. *Journal of Geophysical Research*
722 108(A4), 1141, doi:10.1029/2002JA009543.

723 Robinson, T.R., 1989. The heating of the high latitude ionosphere by high power radio waves.
724 *Physics Reports* 179, 79 – 209.

725 Robinson, T.R., Stocker, A.J., Bond, G.E., Eglitis, P., Wright, D.M., Jones T.D., 1997. O-and X-
726 mode heating effects observed simultaneously with the CUTLASS and EISCAT radars and
727 low power HF diagnostic at Tromsø. *Annales Geophysicae* 15, 134 - 136.

728 Stubbe, P., Kohl, H., Rietveld, M.T., 1992. Langmuir turbulence and ionospheric modification.
729 *Journal of Geophysical Research* 97, 6285 – 6297.

730 Stubbe P., 1996. Review of ionospheric modification experiments at Tromsø. *Journal of*
731 *Atmospheric and Solar-Terrestrial Physics* 58, 349 – 368.

732 Thidé, B., Kopka, H., Stubbe, P., 1982. Observations of stimulated scattering of a strong high
733 frequency radio wave in the ionosphere. *Physics Review Letters* 49, 1561 – 1564.

734 Vas'kov, V.V., Ryabova, N.A., 1998. Parametric excitation of high frequency plasma
735 oscillations in the ionosphere by a powerful extraordinary radio wave. *Advances in Space*
736 *Research* 21, 697 – 700.

737

738 Figure captions

739

740 Figure 1. EISCAT UHF radar observations in the magnetic zenith (13°S) obtained with 30 s
741 integration time during HF modification experiment at Tromsø on 3 November 2013 from 15.30
742 – 18 UT. Altitude-temporal variations of the electron density (a), temperature (b), ion velocities
743 (c), and variations in time at fixed altitudes of the electron density (d) and temperature (e). High-
744 power HF radio waves with alternating O/X polarization were transmitted along the magnetic
745 field line at frequency of 6.2 MHz by pulses of 10 min on, 5 min off. Effective radiated power is
746 about of 450 MW. The heater pulses and polarization of HF pump wave are drawn on the time
747 axis of the bottom plot.

748

749 Figure 2. CUTLASS (SuperDARN) radar observations at Hankasalmi, Finland, at frequencies of
750 about 13, 16, and 18 MHz, by using the single beam 5 directed over Tromsø, on 3 November
751 2013 from 15.30 – 18 UT. Backscatter averaged over the HF-induced ionosphere patch (top
752 panel) and backscatter at every frequency in the dependence on distance (range gate) and time
753 (bottom panels). The features of HF heater transmission are the same as in Fig. 1

754

755 Figure 3. EISCAT UHF radar observations in the magnetic zenith (13°S) in the course of HF
756 modification experiment at Tromsø on 28 October 2013 from 15.30 – 17.45 UT. Behavior in
757 time of undecoded plasma line powers (a), altitude distribution of downshifted plasma line
758 intensities (b), altitude distribution of raw electron densities, or backscattered powers (c), and
759 critical frequencies of the F2 layer, foF2 (d). High-power HF radio waves with X polarization
760 were transmitted along the magnetic field line at frequency of 6.96 MHz by pulses of 10 min on,
761 5 min off. Effective radiated power was about of 550 MW. The heater pulses are drawn on the
762 time axis.

763

764 Figure 4. The maximum power of HF-enhanced downshifted plasma lines, upshifted and
765 downshifted ion lines against the altitude during HF pulses from 15.31 – 15.41 UT at 15.32,
766 15.34, 15.36, 15.38, and 15.40 UT, when $f_H / foF2 < 1$ (a) and from 16.31 – 16.41 UT at 16.32,
767 16.34, 16.36, 16.38, and 16.40 UT, when $f_H / foF2 > 1$ (b) in the course of the X-mode
768 experiment on 28 October 2013. The power spectra were calculated with integration time of 30 s
769 and height resolution of 3 km from the “raw” data obtained with the EISCAT UHF radar at
770 Tromsø. The details of HF heater transmission are the same as in Fig. 3.

771

772 Figure 5. CUTLASS (SuperDARN) radar observations at Hankasalmi, Finland, at frequencies of
773 about 16, 18, and 20 MHz, by using the only beam 5 directed over Tromsø, on 28 October 2013
774 from 15.30 – 18 UT. Backscatter averaged over the HF-induced ionosphere patch (top panel) and
775 backscatter at every frequency in the dependence on distance (range gate) and time (bottom
776 panels). The features of HF heater transmission are the same as in Fig. 3. The heater pulses are
777 drawn on the time axis.

778

779 Figure 6. EISCAT UHF radar observations under elevation angle stepping between 74 and 86° in
780 the course of HF modification experiment at Tromsø on 2 November 2013 from 14.30 – 15 UT,
781 when the heater frequency exceeded the critical frequency of the foF2. Behavior in time of
782 undecoded plasma line powers at the heights of 209 – 383 km (top panel) and the altitude
783 distribution of raw electron densities, or backscattered powers (bottom panel). High-power HF
784 radio waves with X polarization were transmitted along the magnetic field line at frequency of
785 6.96 MHz from 14.31 – 14.51 UT. Effective radiated power was about of 550 MW. During HF
786 pump pulse the UHF radar elevation angle was changed every 2 min in an orderly sequence of
787 74, 76, 77, 78, 79, 80, 82, 84, and 86°. The UHF radar elevation angles are shown on the time
788 axis.

789

790 Figure 7. The ion line spectra depending on the altitude from the EISCAT UHF radar
791 measurements on 2 November 2013 for radar elevation angles of 76, 77, 78, and 79° within the
792 HF pump pulse from 14.31 – 14.51 UT. The ion line spectra were calculated with integration
793 time of 30 s and height resolution of 3 km from the “raw” data obtained with the EISCAT UHF
794 radar at Tromsø. The features of HF heater transmission are the same as in Fig. 6.

795

796 Figure 8. The spectrogram of the heater signal within 100 Hz received near St. Petersburg at a
797 distance about 1200 km away from Tromsø (top panel) and spectrogram of the “classic” SEE in
798 the 200 kHz frequency band recorded near Tromsø (bottom panel) during the alternating O/X
799 mode HF pumping on 21 October 2012 from 14 – 16 UT. High power HF radio wave was
800 injected into the ionosphere at frequency of 7.953 MHz by cycles of 10 min on, 5 min off at
801 three positions of HF beam, such as 90 (vertical), 84 and 78° (magnetic field-aligned). From
802 cycle to cycle the polarization of HF pump wave was changed between O- and X-mode.
803 Effective radiated power was about $ERP = 650$ MW. The heater pulses, HF beam position, and
804 polarization of HF pump wave are shown on the time axis of the top panel.

805

806 Figure 9. The spectrogram of the heater signal within 600 Hz of pump frequency recorded near
807 St. Petersburg for alternating O/X-mode HF pumping on 27 October 2013 from 12 to 13.30
808 UT(a) and power spectra obtained at 12.32.40, 12.35.40, 12.36.20, and 12.38.10 UT in the
809 course of the X-mode pulse from 12.31 – 12.51 UT(b). HF pump wave was transmitted at
810 frequency of 7.953 MHz by cycles of 20 min on, 10 min off towards the magnetic zenith.
811 Effective radiated power was about $ERP = 650$ MW. The heater pulses and polarization of HF
812 pump wave are shown on the time axis of the top panel.

813

814 Figure 10. The spectrogram of the heater signal within 400 Hz of pump frequency recorded near
815 St. Petersburg for X-mode HF pumping on 28 October 2013 from 17 to 18 UT(a) and power

816 spectra obtained at 17.03.30, 17.05.40, 17.08, and 17.09.20 UT in the course of the pulse from
817 17.01 – 17.11 UT(b). The features of HF heater transmission are the same as in Fig. 3. The
818 heater pulses are shown on the time axis of the top panel.
819
820



EISCAT Scientific Association

EISCAT UHF RADAR
3 November 2013

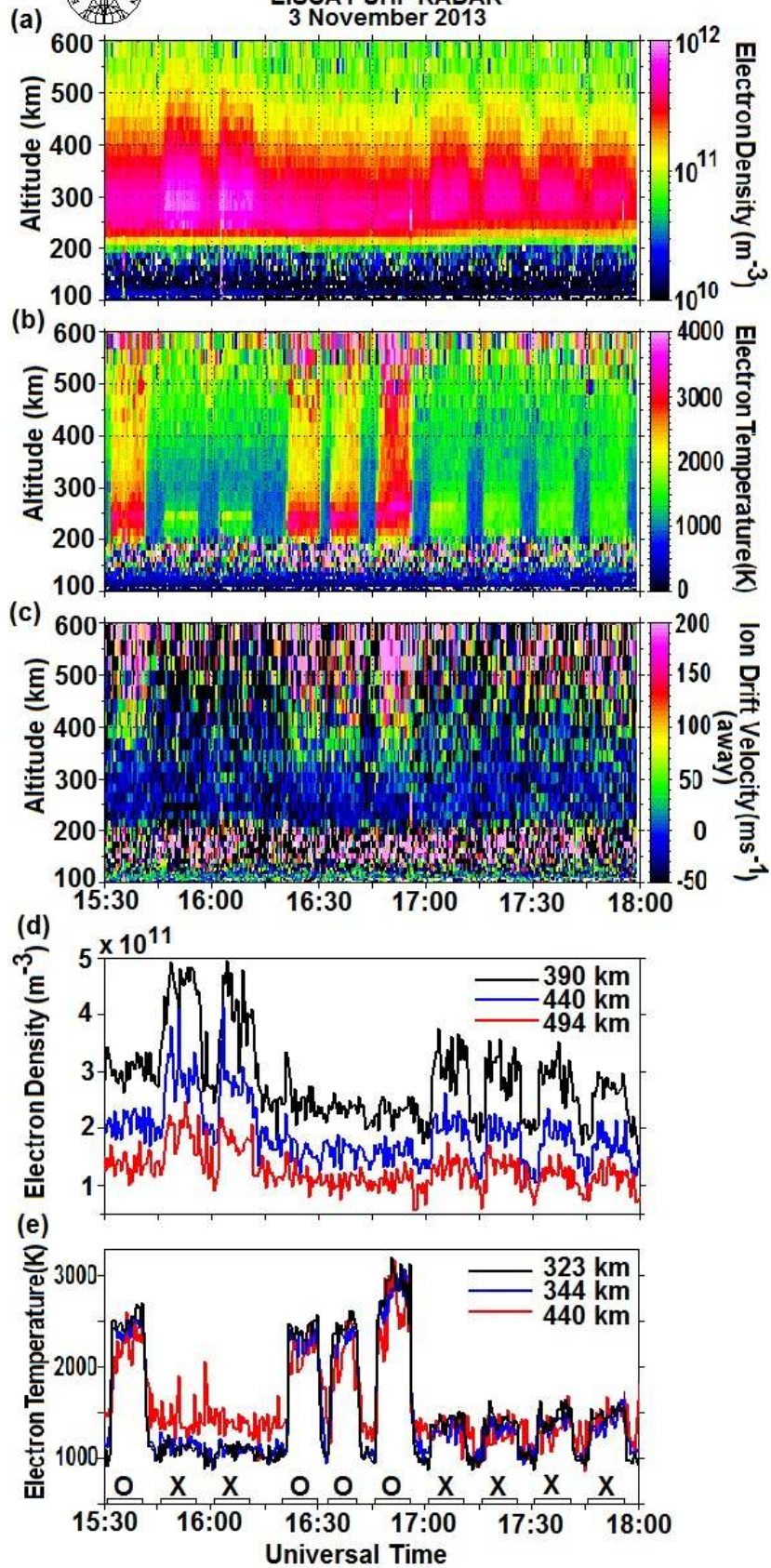


Figure 1.

SUPERDARN PARAMETER PLOT

Hankasalmi: Beam 5

3 Nov 2013

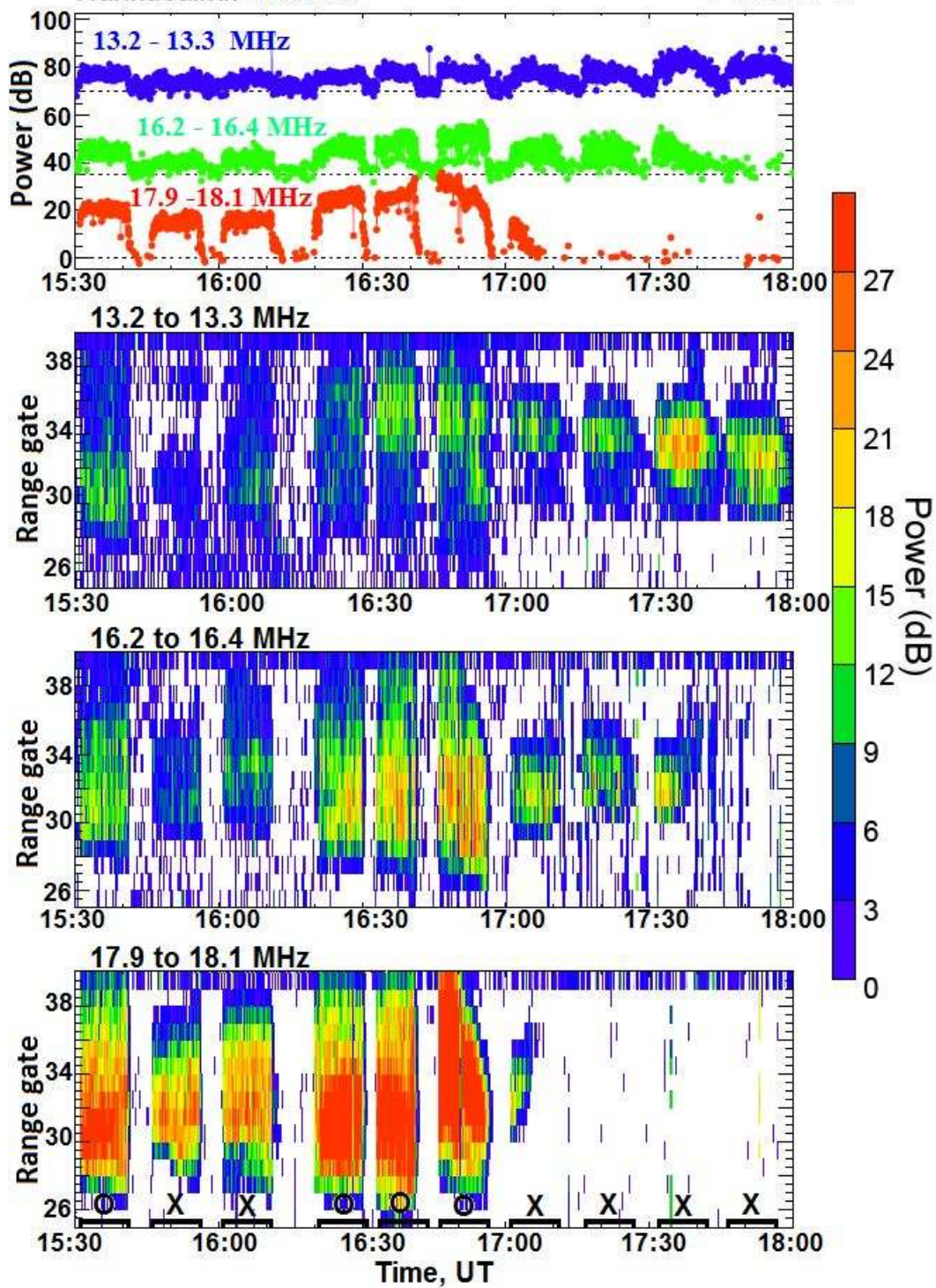


Figure 2.



EISCAT Scientific Association

EISCAT UHF RADAR

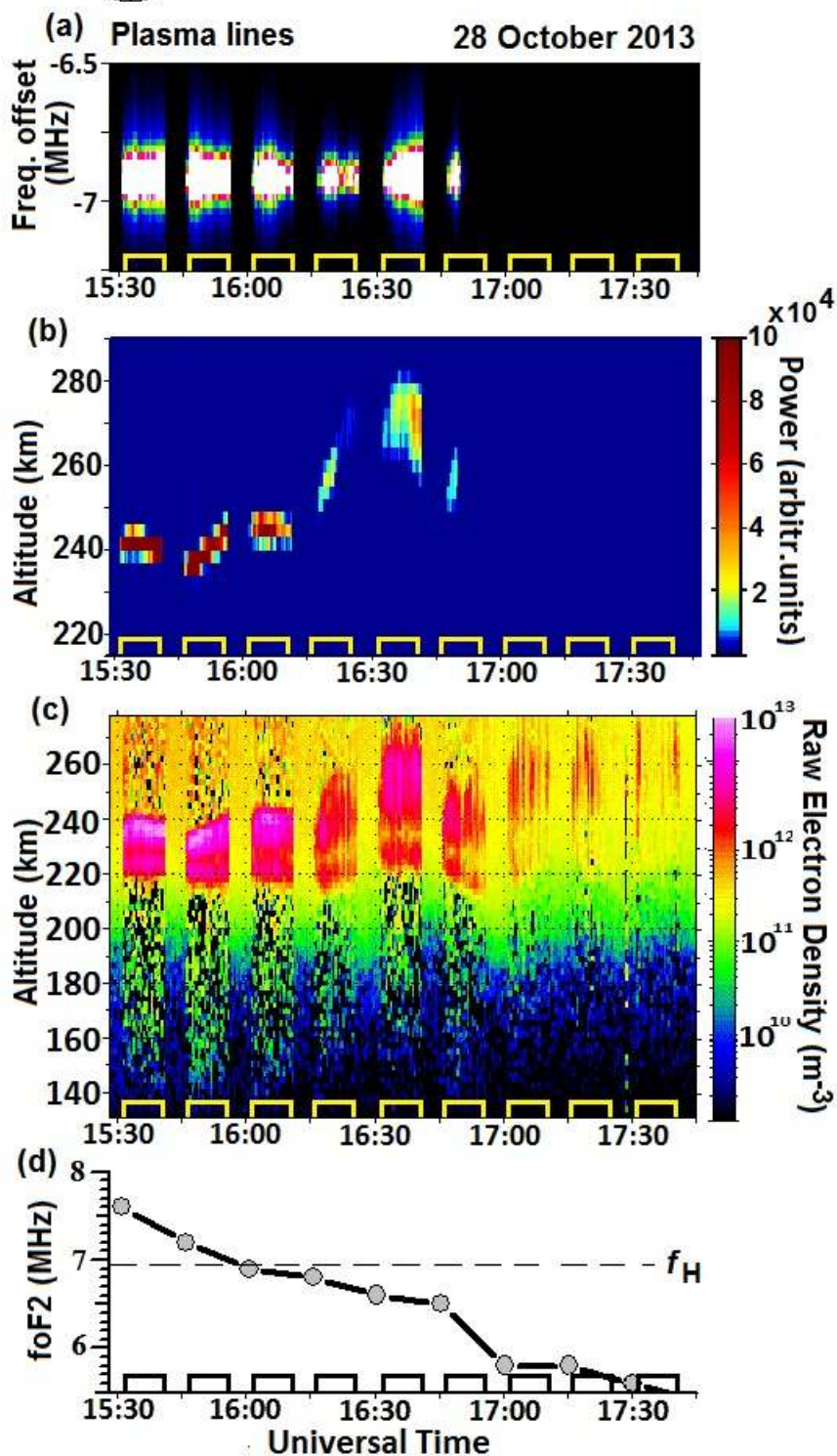


Figure 3.

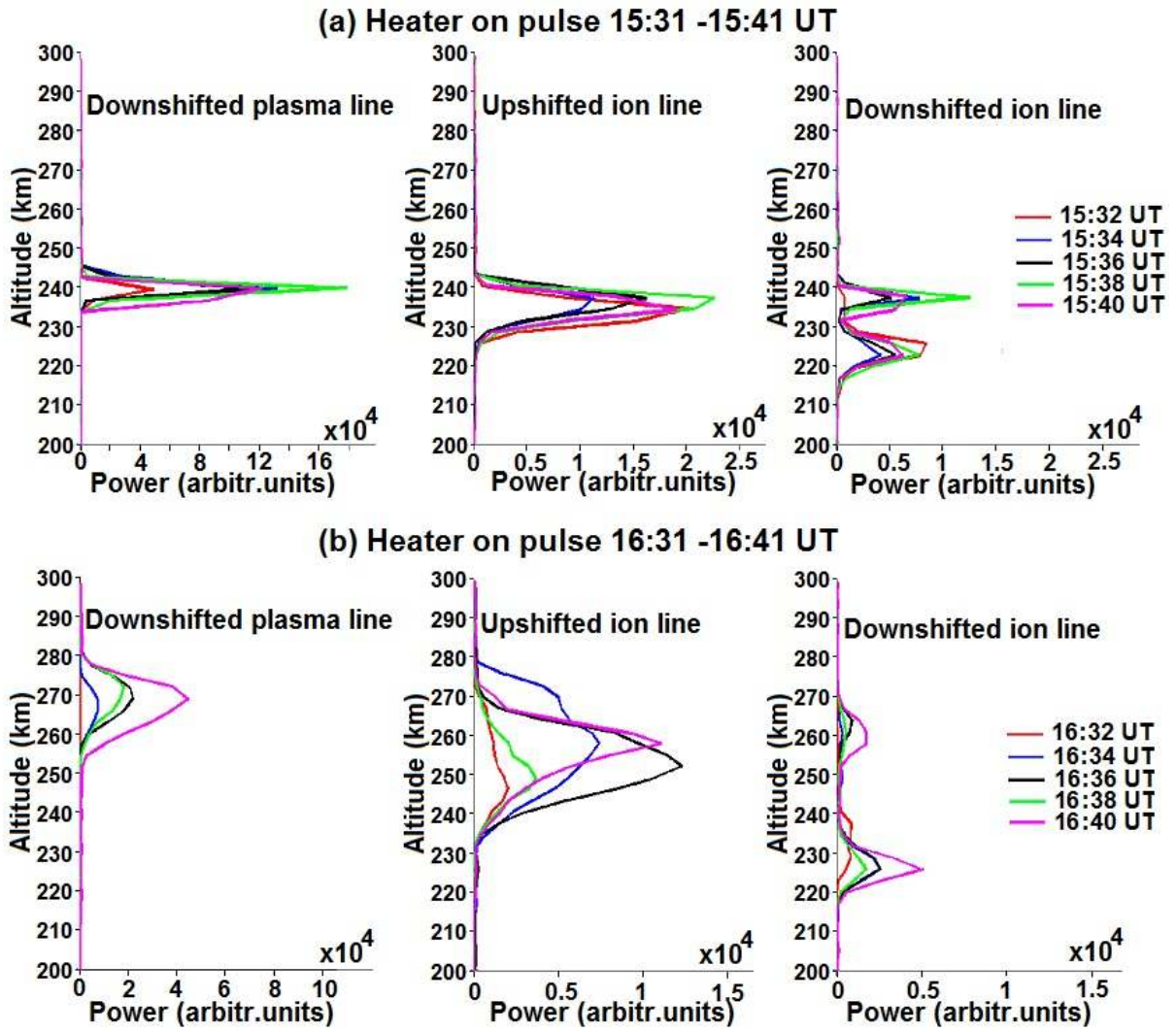


Figure 4.

SUPERDARN PARAMETER PLOT

Hankasalmi Beam 5

28 Oct 2013

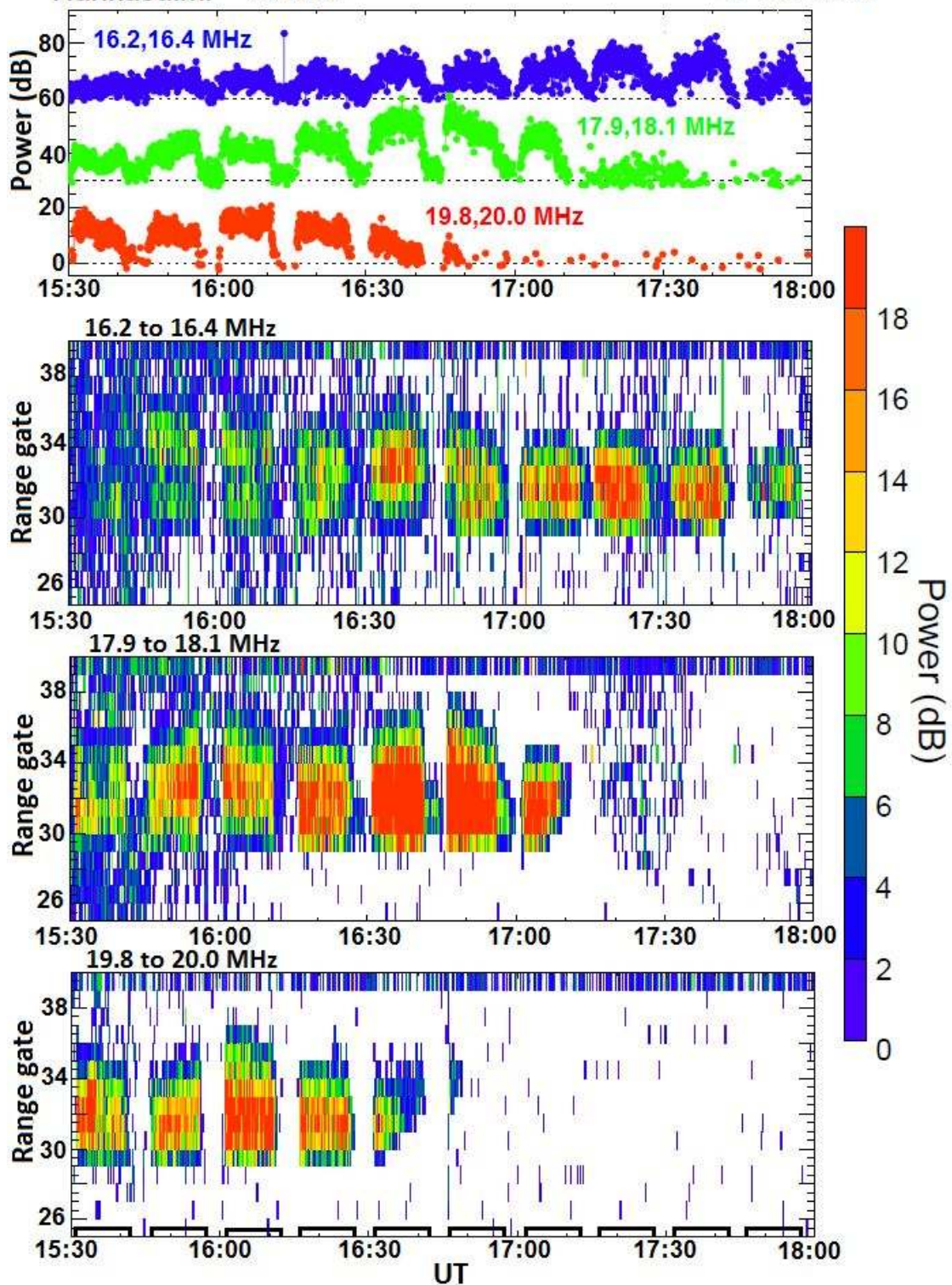


Figure 5.



EISCAT Scientific Association

EISCAT UHF RADAR
2 November 2013

Range 209-383 km

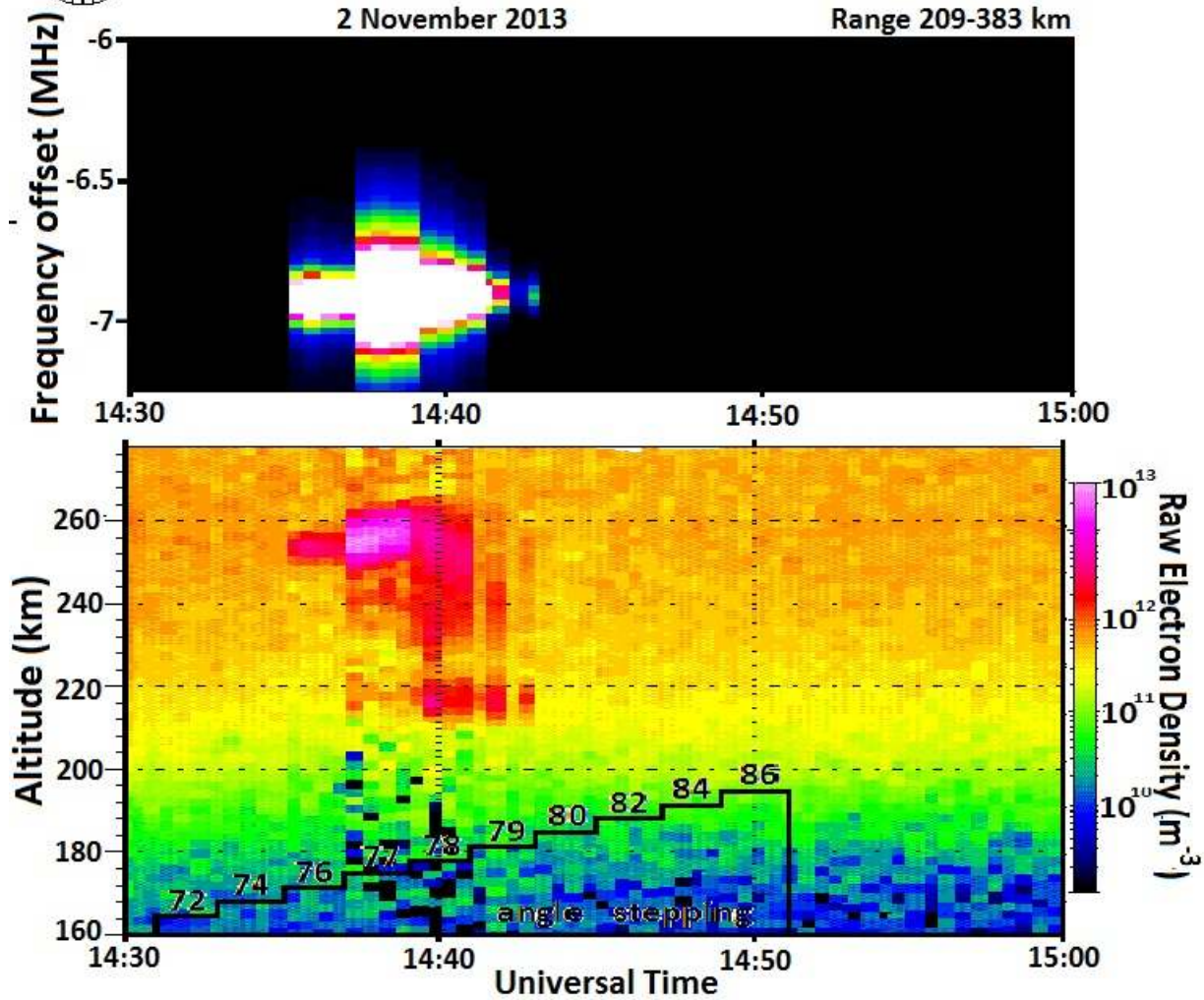


Figure 6.

2 November 2013 14:31 - 14:51 UT, X-mode

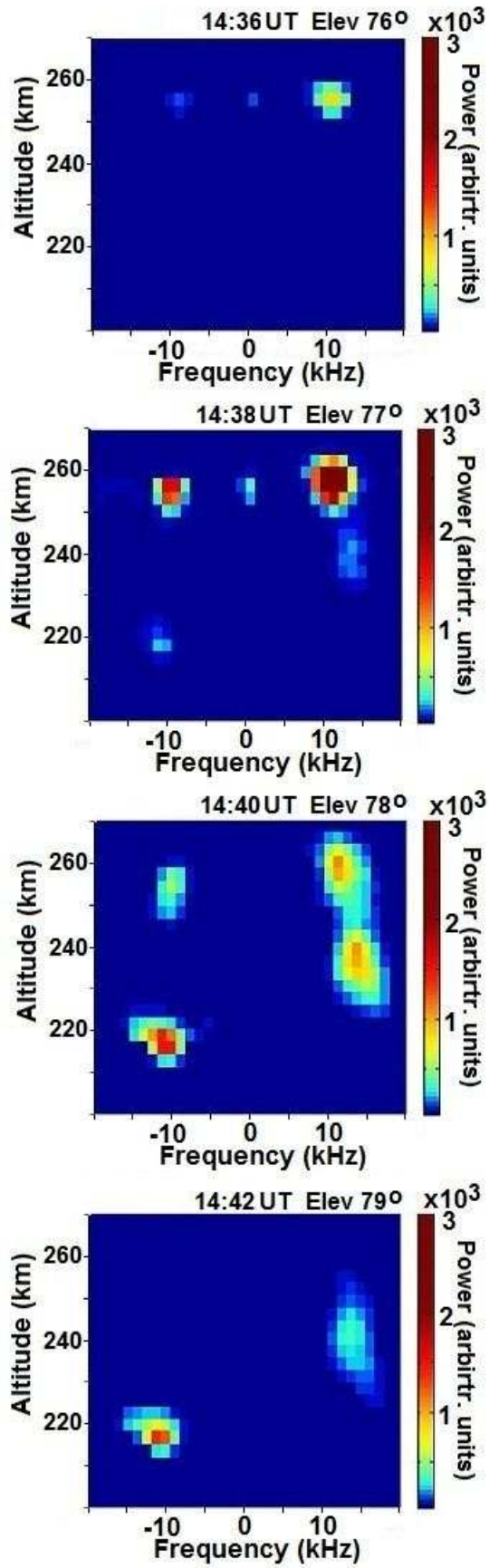


Figure 7.

21 October 2012
Tromsø - S.Petersburg, fH = 7953 kHz

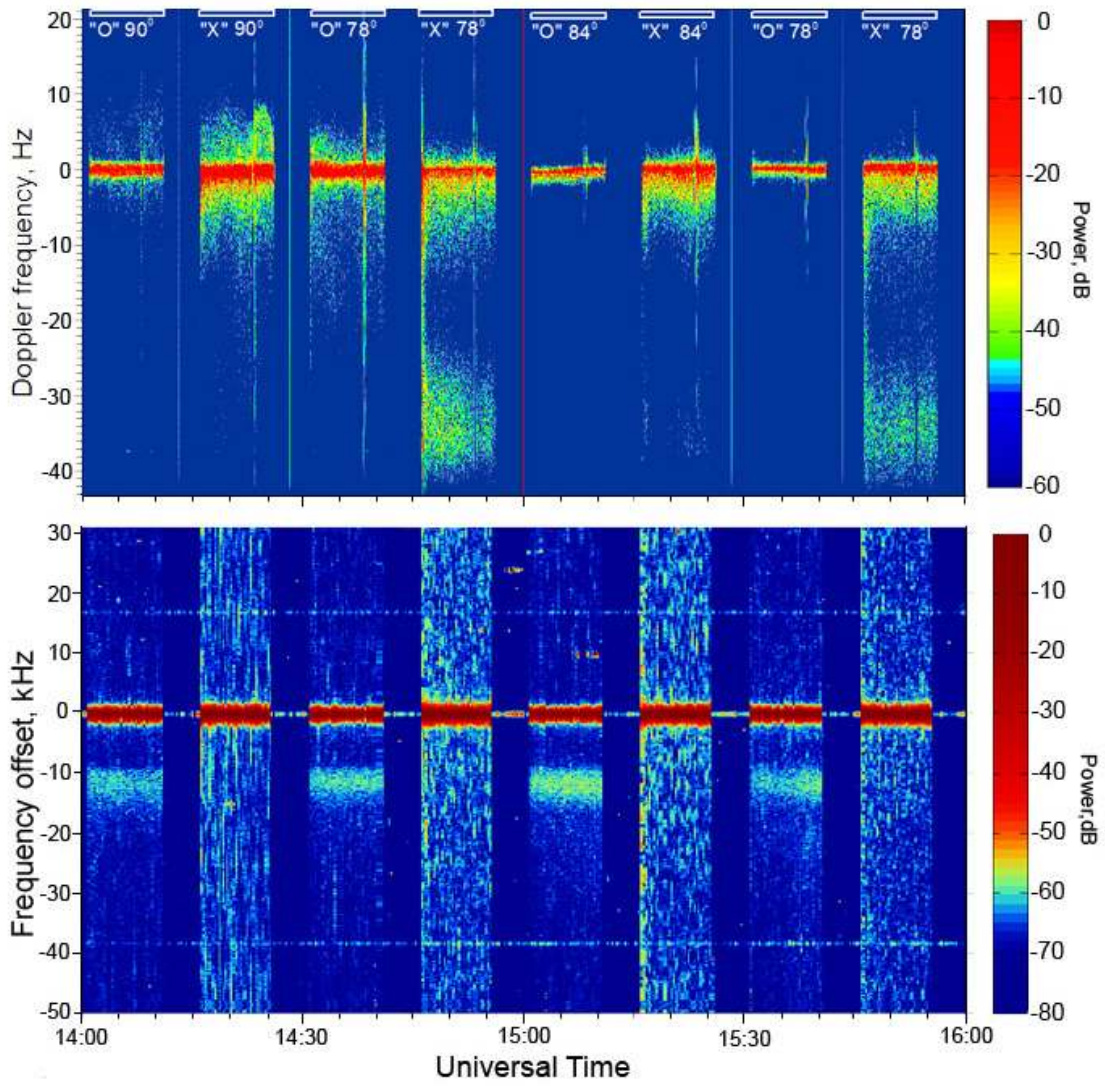


Figure 8.

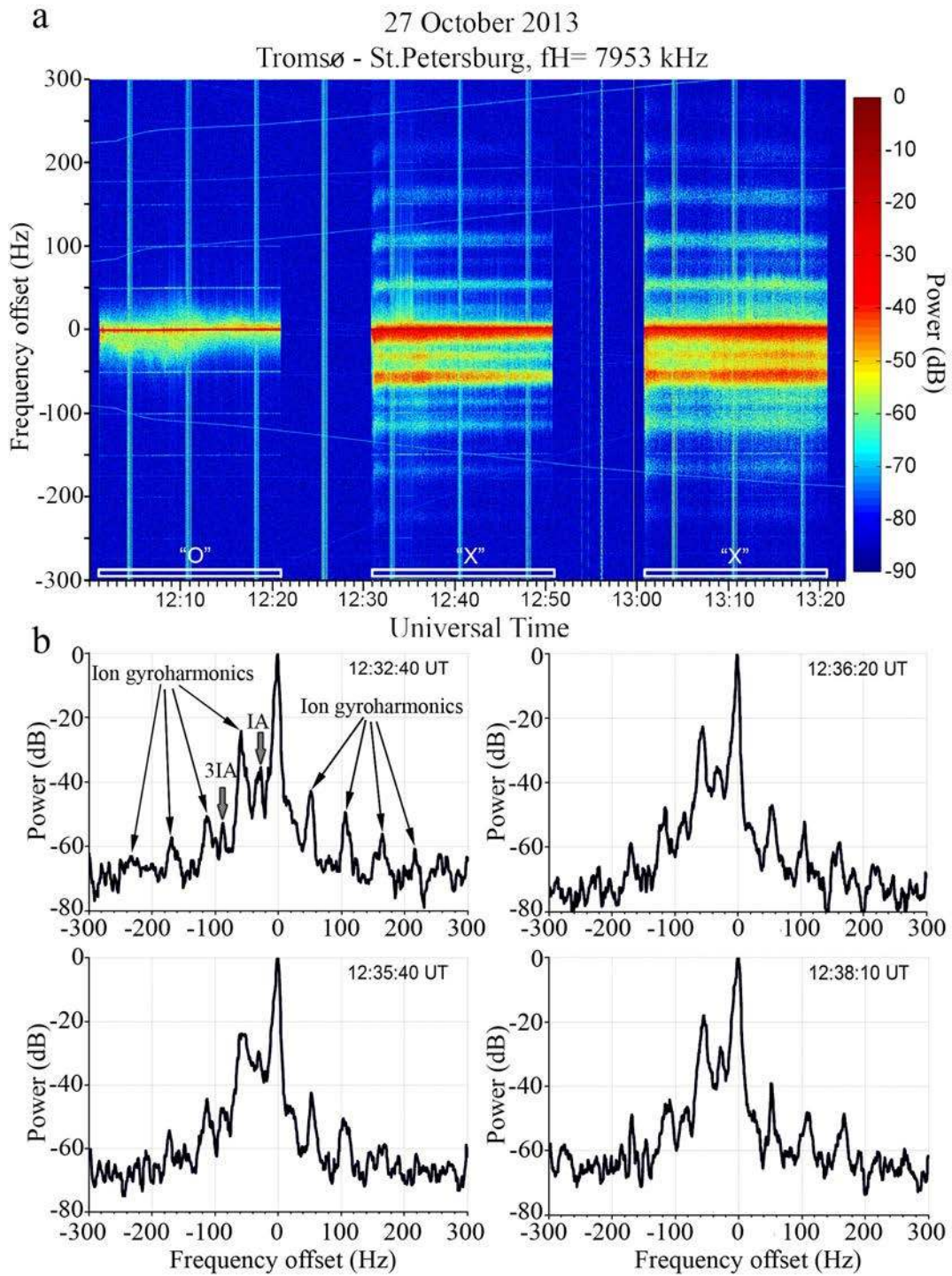


Figure 9.

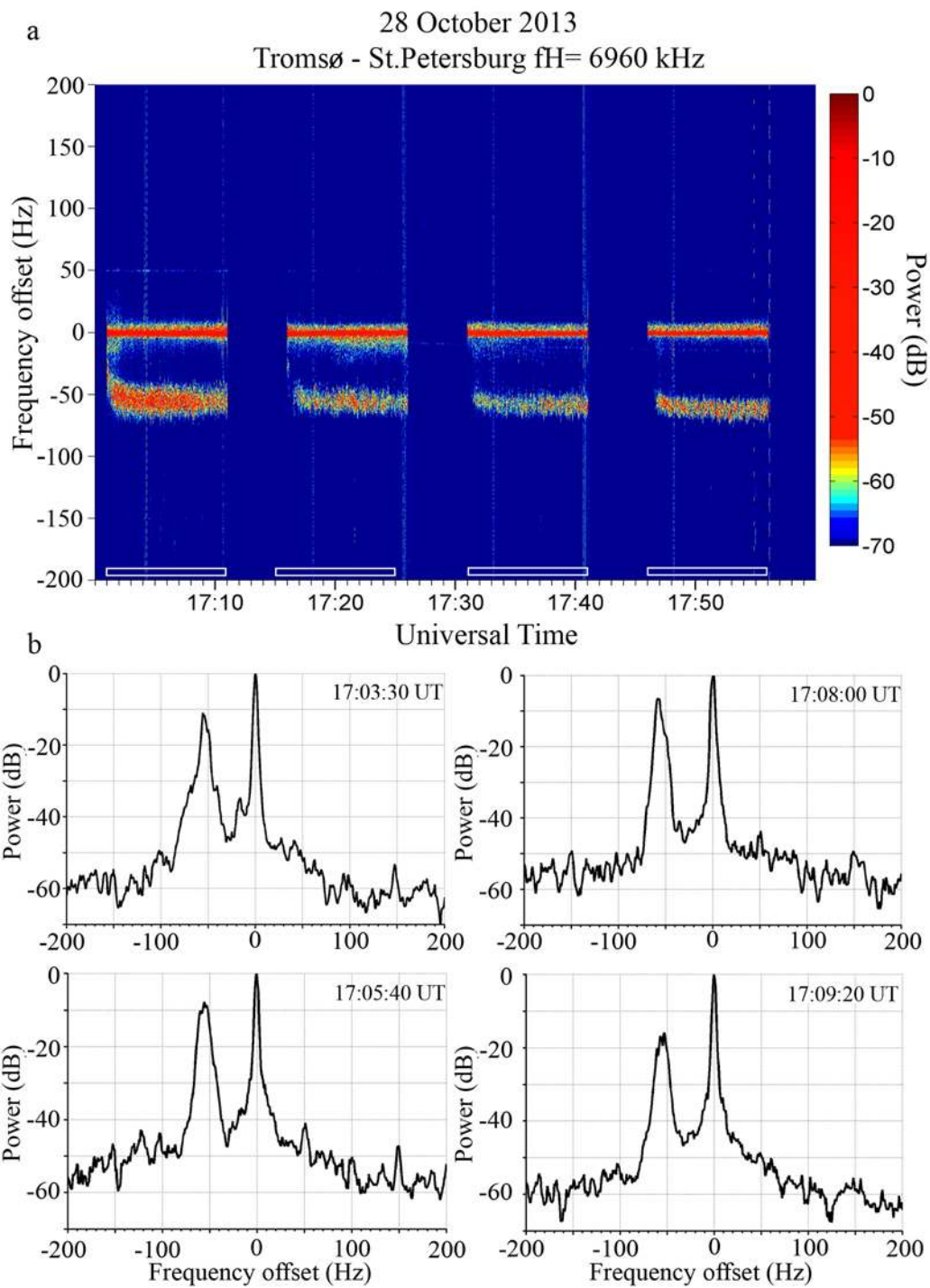


Figure 10.